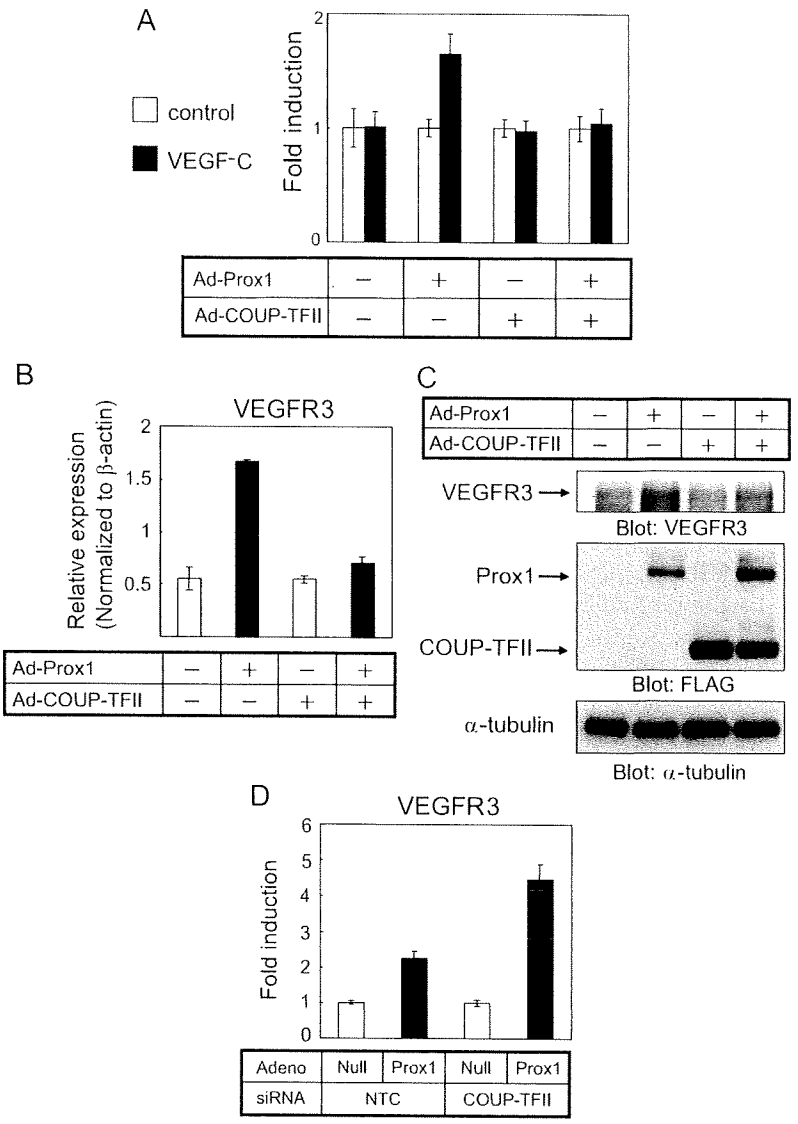

Figure 3 COUP-TFII represses Prox1-induced endothelial cell migration towards VEGF-C via regulation of VEGFR3 expression. (A) Effect of COUP-TFII on the Prox1-induced endothelial cell migration towards VEGF-C. Migration of HUVECs infected with indicated adnoviruses was measured by Boyden chamber assay as described previously (Mishima *et al.* 2007). Relative migration towards VEGF-C is shown as a ratio of the number of migrated cells in the presence of VEGF-C against that in the absence of VEGF-C. Bars, SD. (B–C) Effect of gain-of-function of COUP-TFII on the Prox1-induced expression of VEGFR3. HUVECs were infected with indicated adenoviruses, followed by quantitative RT-PCR (B) and Western blotting (C: top panel) for VEGFR3. Western blotting was also carried out for FLAG-tagged Prox1 and COUP-TFII transduced by adenoviruses (middle panel). α-tubulin was used as a loading control (bottom panel). (D) Effect of loss-of-function of COUP-TFII on the Prox1-induced expression of VEGFR3. HUVECs were infected with adenovirus coding for Prox1 (Ad-Prox1) or non-conding adenovirus (Ad-Null) in combination with siRNA for COUP-TFII or negative control siRNA (NTC), followed by quantitative RT-PCR for VEGFR3. Bars, SD.

when COUP-TFII expression was knocked down in HUVECs, induction of VEGFR3 expression by Prox1 was enhanced (Fig. 3D). These results suggest that COUP-TFII suppresses Prox1-induced endothelial chemotaxis towards VEGF-C by regulating VEGFR3 expression.

Endogenous level of COUP-TFII expression in HDLECs is required to maintain the expression of VEGFR3

We next investigated the roles of COUP-TFII in the LECs in which endogenous Prox1 is expressed. When the level of COUP-TFII expression was elevated in HDLECs, both proliferation (Fig. 4A) and chemotaxis towards VEGF-C (Fig. 4C) were suppressed with concomitant decrease in the expression of cyclin E1 (Fig. 4B) and VEGFR3 (Fig. 4D). These findings were consistent with the results observed in HUVECs. However, when COUP-TFII was knocked down in HDLECs, their migration towards VEGF-C and VEGFR3 expression were attenuated (Fig. 4E,F), whereas neither cell number nor cyclin E1 expression changed (data not shown). These results suggest that COUP-TFII differentially functions between HDLECs and HUVECs.

We further examined whether COUP-TFII alters the endogenous Prox1 expression in LECs. As shown in Fig. 4G, endogenous Prox1 expression was significantly decreased when the level of COUP-TFII expression was

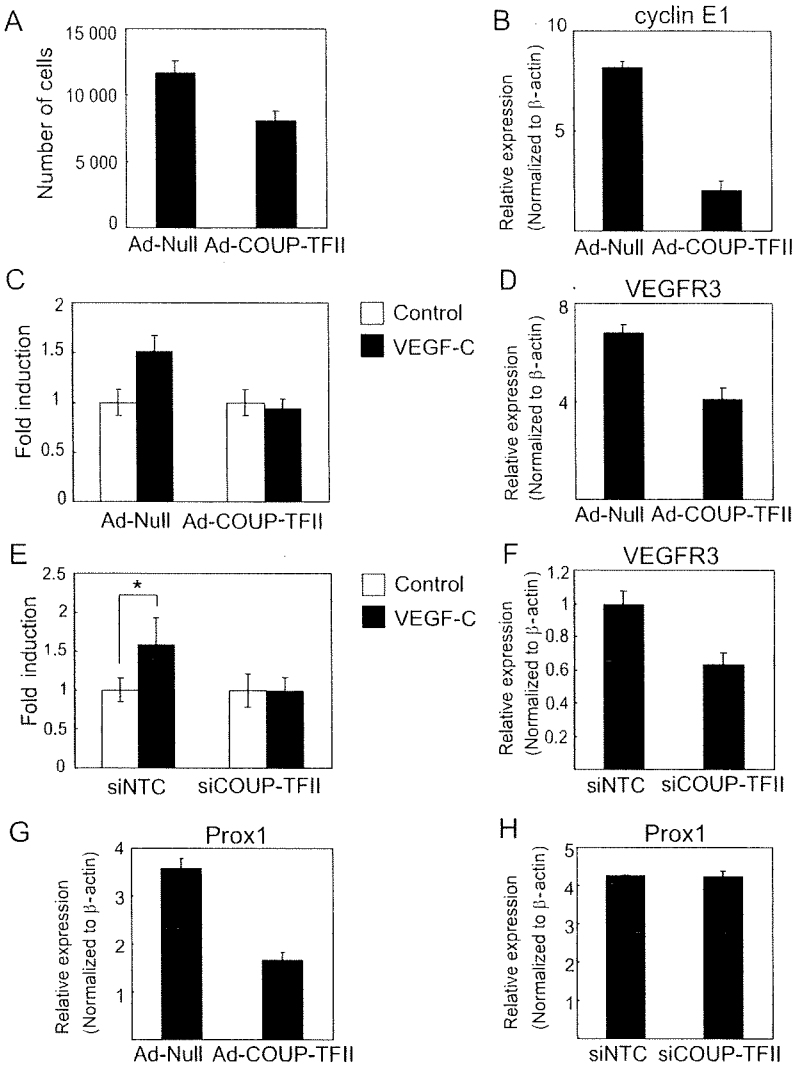

Figure 4 Endogenous level of COUP-TFII expression plays important roles in the maintenance of characteristics of HDLECs. (A–D) HDLECs infected with non-coding adenovirus (Ad-Null) or adenovirus coding for COUP-TFII (Ad-COUP-TFII) were subjected to cell proliferation assay (A), chamber migration assay using VEGF-C as an attractant (C) and quantitative RT-PCR analyses for cyclin E1 (B) and VEGFR3 (D). (E, F) HDLECs transfected with control siRNA (siNTC) or siRNA for COUP-TFII (siCOUP-TFII) were subjected to chamber migration assay using VEGF-C as an attractant (E) and quantitative RT-PCR analyses for VEGFR3 (F). In (C) and (E), relative migration towards VEGF-C is shown as a ratio of the number of migrated cells in the presence of VEGF-C against that in the absence of VEGF-C. (G, H) Expression of endogenous Prox1 expression was determined in the HDLECs infected with Ad-COUP-TFII (G) or transfected with siCOUP-TFII (H). $*P < 0.01$. Bars, SD.

elevated in HDLECs, while the loss of COUP-TFII expression did not alter the Prox1 expression (Fig. 4H). These results suggest that excessive level of COUP-TFII may interfere with the functions of Prox1 directly by inhibiting the transcriptional activities of Prox1 and indirectly by suppressing the endogenous Prox1 expression.

COUP-TFII interacts with Prox1 in HDLECs

Previous reports that LRH-1 and SF-1, members of nuclear receptor superfamily, bind Prox1 (Qin *et al.* 2004; Steffensen *et al.* 2004) prompted us to examine whether COUP-TFII and Prox1 interact. We carried out co-immunoprecipitation experiments with cell lysates prepared from the HUVECs infected with adenoviruses coding for Prox1 and COUP-TFII (Fig. 5A). When the lysates were subjected to immunoprecipitation, we detected COUP-TFII in the immunoprecipitates pulled down with anti-Prox1 antibody, which indicates that Prox1 is capable of interacting with COUP-TFII in HUVECs.

Next, we examined whether endogenous Prox1 and COUP-TFII interact in HDLECs using the Duolink *in situ* proximity ligation assay (PLA). This method enables us to monitor subcellular localization of endogenous protein–protein interactions at single molecule resolution (Söderberg *et al.* 2006, 2008). In the HUVECs infected with adenoviruses coding for Prox1 and COUP-TFII, we detected a number of strong fluorescence signals in the presence of specific antibodies, which indicates the interaction between Prox1 and COUP-TFII in the

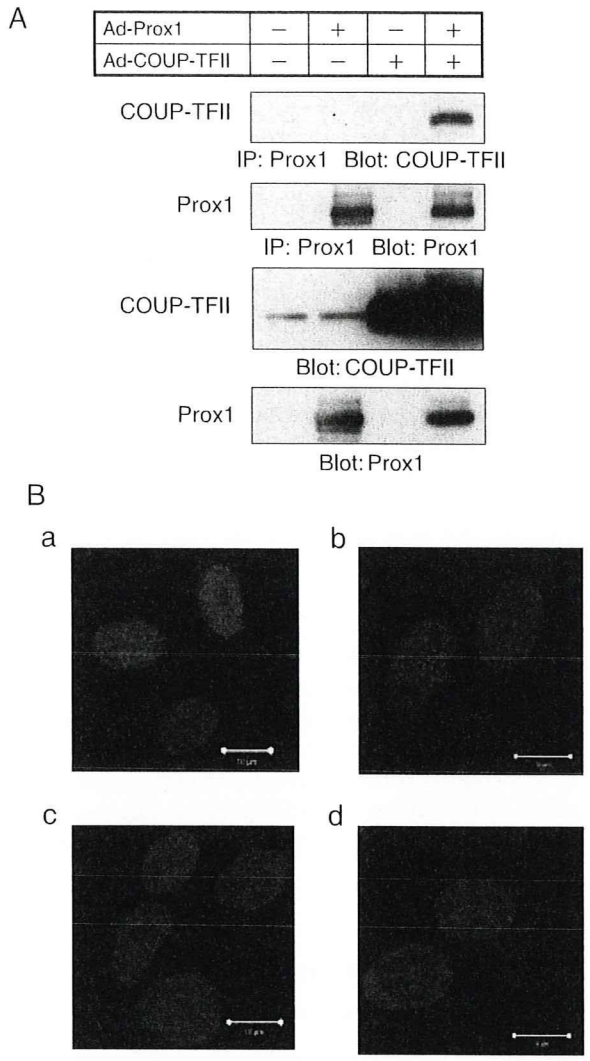

Figure 5 COUP-TFII physically interacts with Prox1. (A) Co-immunoprecipitation of COUP-TFII with Prox1 in HUVECs. HUVECs infected with adenovituses coding for Prox1 (Ad-Prox1) and COUP-TFII (Ad-COUP-TFII) were subjected to immunoprecipitation with anti-Prox1 antibody, followed by immunoblotting with anti-COUP-TFII antibody (top panel). Expression of Prox1 and COUP-TFII was also confirmed. (B) Interaction of endogenous Prox1 and COUP-TFII in HDLECs. PLA was carried out to detect the proximal location of Prox1 and COUP-TFII (shown as red dots) as described in Experimental Procedures. All samples were counterstained with TOTO3 (blue) to visualize nuclei. (a–c) HUVECs infected with adenoviruses coding for Prox1 and COUP-TFII (a), native HDLECs (b) and native HUVECs (c) were subjected to PLA after treating with antibodies for Prox1 and COUP-TFII. Note that specific interaction between Prox1 and COUP-TFII is detected in the nuclei only when Prox1 and COUP-TFII are present. (d) Native HDLECs were subjected to PLA without treating with antibodies for Prox1 and COUP-TFII. Scale bars, 10 μm.

nuclei (Fig. 5Ba), whereas no signals were detected in native HUVECs in the presence of specific antibodies (Fig. 5Bc) or in HDLECs in the absence of specific antibodies (Fig. 5Bd). In the native HDLECs, we could detect definite fluorescence signals restricted to the nuclei in the presence of specific antibodies (Fig. 5Bb), suggesting that endogenous Prox1 and COUP-TFII interact in the nuclei of HDLECs. In order to examine the specificity of the signals, we knocked down COUP-TFII expression by siRNA in HDLECs and carried out PLA (Fig. S3 in Supporting Information). The fluorescence signals seen in the HDLECs transfected with control siRNA were significantly decreased by knocking down COUP-TFII expression. These results allowed us to conclude that endogenous COUP-TFII interacts with Prox1 in the nuclei of HDLECs.

COUP-TFII and Prox1 bind to the cyclin E1 promoter

Petrova *et al.* showed that Prox1 activates cyclin E1 promoter whereas Prox1 DNA binding mutant does not (Petrova *et al.* 2002), suggesting that Prox1 may regulate the transcription of cyclin E1 via direct binding to the cyclin E1 promoter. Because COUP-TFII suppresses Prox1-induced cyclin E1 expression and physically interacts with Prox1, we examined whether Prox1 and COUP-TFII bind to the endogenous cyclin E1 promoter in intact chromatin.

Cross-linked chromatin samples prepared from HUVECs infected with adenoviruses coding for Prox1 and COUP-TFII were subjected to chromatin immunoprecipitation (ChIP) assays (Fig. 6). The cyclin E1 promoter region

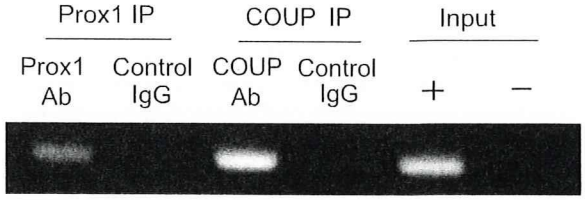

Figure 6 COUP-TFII and Prox1 directly bind to the cyclin E1 promoter. HUVECs infected with adenoviruses coding for Prox1 and COUP-TFII were subjected to ChIP assay. PCR was carried out to detect the cyclin E1 promoter containing putative binding sequences for Prox1 and COUP-TFII. Prox1 Ab and COUP Ab lanes show amplification of target sequences within the immunoprecipitates (IP) using antibodies for Prox1 and COUP-TFII, respectively. Control IgG lanes show PCR amplification of samples precipitated with corresponding control IgG antibodies. Input lanes show amplification of total input DNA (+) or no DNA (–).

containing putative binding consensus sequences for Prox1 and COUP-TFII was pulled down with antibodies for Prox1 and COUP-TFII, suggesting that both Prox1 and COUP-TFII bind to the cyclin E1 promoter.

Discussion

In the present study, we show that COUP-TFII regulates the transcriptional activities of Prox1. In BECs, both gain- and loss-of-function studies showed that COUP-TFII negatively regulates Prox1 to induce the expression of cyclin E1 and VEGFR3. COUP-TFII has been reported to negatively regulate the transcription via binding to the promoter and recruitment of co-repressor complexes containing N-CoR, SMRT and histone deacetylase (HDAC) (Park *et al.* 2003). The present findings that COUP-TFII and Prox1 physically and functionally interact may suggest that positive transcriptional regulation by Prox1 is repressed by the co-repressor complexes that are recruited to the promoter by COUP-TFII.

We also found that endogenous level of COUP-TFII in LECs is required to maintain the expression of VEGFR3, which is not consistent with the results observed in HUVECs. This difference may be caused by the cell type specific contexts of expression of other transcription factors. Additionally, elevation of the level of COUP-TFII expression in LECs also decreased the expression of VEGFR3. We also found that both gain- and loss-of-function of COUP-TFII decreased the expression of LEC markers including integrin α9 and podoplanin and BEC markers including VE-cadherin and VEGFR2 (Fig. S4). These results suggest that a certain range of COUP-TFII expression is required to maintain the expression of a group of LEC and BEC markers. Similar phenomenon is observed in the relationship between the expression of Oct3/4 and maintenance of pluripotency of mouse embryonic stem cells (Niwa *et al.* 2000).

While endothelial markers examined so far appear to require endogenous level of COUP-TFII in HDLECs, we found that not all of endothelial markers are regulated by COUP-TFII in a similar manner. Ablation of COUP-TFII gene in endothelial cells allowed the ectopic expression of ephrin B2 and Neuropilin 1 (NRP1), both of which are arterial endothelial cell markers, in veins (You *et al.* 2005). In accordance with the previous result, COUP-TFII expression decreased ephrin B2 expression while loss-of-COUP-TFII expression increased it in HDLECs (Fig. S4E in Supporting Information). However, to our surprise, both gain- and loss-of-function studies showed that COUP-TFII positively regulates NRP1 expression in HDLECs (Fig. S4F in Supporting Information). Molecular mechanisms of how COUP-TFII differentially regulates the transcription of various target genes between BECs and LECs remain to be investigated in the future.

During embryonic lymphatic development, Prox1 expressing BECs in veins differentiate into LECs and sprout out to form primary lymphatic plexus (Oliver 2004). While we showed that COUP-TFII is expressed in HDLECs at lower level than in HUVECs, it remains to be elucidated how COUP-TFII expression is regulated during lymphatic development in embryos. Loss-of-function studies show that COUP-TFII negatively and positively regulates the VEGFR3 expression in BECs and LECs, respectively. These results may suggest that COUP-TFII maintains the identity of venous endothelial cells by inhibiting Prox1-mediated VEGFR3 expression in BECs, but aids in maintaining VEGFR3 expression in LECs. This differential transcriptional regulation by COUP-TFII may play important roles in segregating lymphatics from veins during formation of primary lymphatic plexus.

As Prox1 plays critical roles in the formation and maintenance of lymphatic vessels (Mishima *et al.* 2007), regulation of transcriptional activities of Prox1 will aid in manupilating lymphangiogenesis in pathological situations. While ligands for COUP-TFII receptor have not yet been identified, better understanding of the regulation of the COUP-TFII may be useful for developing therapeutic strategies to treat lymphedema and tumor lymphangiogenesis in the future.

Experimental procedures

Cell culture and adenovirus production

HUVECs and HDLECs were purchased from Sanko Junyaku and TaKaRa, and cultured in endothelial basal medium (EBM) containing 2% and 5% fetal bovine serum (FBS), respectively, supplemented with endothelial cell growth supplement (TaKaRa). Recombinant adenoviruses coding for mouse Prox1 and mouse COUP-TFII were generated and used as described (Shirakihara *et al.* 2007).

RNA interference and oligonucleotides

siRNAs were introduced into cells using HiperFect' reagent (QIAGEN) according to the manufacturer's instructions. The COUP-TFII siRNA (SI00128814) and the negative control siRNA were obtained from QIAGEN.

Immunohistochemistry and Western blot analysis

Immunostaining was carried out with anti-Prox1 (1 : 100 dilution; Abcam), anti-COUP-TFII (1 : 100 dilution; Perseus Proteomics)

and anti-LYVE-1 (1 : 200 dilution; Abcam) antibodies, followed by counterstaining with TOTO3 (Invitrogen–Molecular Probes). Stained specimens were examined using a LSM 510 META confocal microscope (Carl Zeiss). All images were imported into Adobe Photoshop as JPEGs or TIFFs for contrast manipulation and figure assembly. Antibodies to FLAG and α-tubulin for Western blot analysis were obtained from SIGMA. Antibody to human VEGFR3 for Western blot analysis was obtained from Santa Cruz. Western blot analysis was carried out as described (Watabe *et al.* 2003).

Proximity ligation assay (PLA)

The Duolink *in situ* PLA kits were purchased from Olink (http://www.olink.com/). Fixation of the cells, blocking of non-specific binding of antibody, and immunostaining using anti-Prox1 (Abcam) and anti-COUP-TFII (Perseus Proteomics) were carried out as described above. Subsequently, a pair of secondary antibodies conjugated with oligonucleotides (PLA probes) was used according to the manufacturer's protocol to generate fluorescence signals only when the two PLA probes were in close proximity (40 nm). The fluorescence signal from each detected pair of PLA probes was visualized as a distinct individual dot (Söderberg *et al.* 2006, 2008). Nuclei counterstaining and analysis of the images were carried out as described earlier.

Isolation of RNA and quantitative RT-PCR

Total RNAs were extracted from HUVECs and HDLECs using the RNeasy Mini Kit (QIAGEN). First-strand cDNAs were synthesized by SuperScriptIII reverse transcriptase (Invitrogen) using random hexamer primers according to the manufacturer's instruction. Quantitative RT-PCR analyses were carried out using the ABI PRISM 7500 Fast Real-Time PCR System (Applied Biosystems) and Power SYBR Green PCR master mix (Applied Biosystems). All expression data were normalized to those for β-actin. In the cases when siRNAs and adenoviruses were simultaneously used, expression data are presented as a ratio of the expression level in the samples infected with adenovirus coding for Prox1 against those with non-coding adenovirus. The primer sequences are available online as indicated in Table S1 in Supporting Information.

Chamber migration assay

Migration assay was carried out as described previously (Mishima *et al.* 2007). As a chemoattractant, 100 ng/mL and 300 ng/mL of recombinant VEGF-C (Calbiochem) were used for HDLECs and HUVECs, respectively.

ChIP assays

HUVECs infected with adenoviruses were fixed by adding formaldehyde and harvested. In order to precipitate Prox1 and COUP-TFII, anti-Prox1 antibody (R&D) and anti-COUP-TFII (Perseus Proteomics) were used. PCR of the cyclin E1 promoter containing putative binding sites for Prox1 and COUP-TFII was done using immunoprecipitated chromatin with the following pair of oligonucleotide primers:

5′-ACCAGCCTGAGCAACATAGCA-3′ and 5′-CAGTGAG ACCCCCATTTCTACA-3′.

Acknowledgements

Authors thank Drs. M. Tsai and S. Tsai for COUP-TFII cDNA, Ms. M. Arase for technical assistance, Drs. T. Minami, T. Kodama, and members of Department of Molecular Pathology of the University of Tokyo for discussion. This research was supported by Grants-in-Aid for Scientific Research from the Ministry of Education, Culture, Sports, Science and Technology of Japan.

References

Cao, R., Björndahl, M.A., Religa, P., Clasper, S., Garvin, S., Galter, D., Meister, B., Ikomi, F., Tritsaris, K., Dissing, S., Ohhashi, T., Jackson, D.G. & Cao, Y. (2004) PDGF-BB induces intratumoral lymphangiogenesis and promotes lymphatic metastasis. *Cancer Cell* **6**, 333–345.

Cui, W., Tomarev, S.I., Piatigorsky, J., Chepelinsky, A.B. & Duncan, M.K. (2004) Mafs, Prox1, and Pax6 can regulate chicken βB1-crystallin gene expression. *J. Biol. Chem.* **279**, 11088–11095.

He, Y., Kozaki, K., Karpanen, T., Koshikawa, K., Yla-Herttuala, S., Takahashi, T. & Alitalo, K. (2002) Suppression of tumor lymphangiogenesis and lymph node metastasis by blocking vascular endothelial growth factor receptor 3 signaling. *J. Natl Cancer Inst.* **94**, 819–825.

Jeltsch, M., Kaipainen, A., Joukov, V., Meng, X., Lakso, M., Rauvala, H., Swartz, M., Fukumura, D., Jain, R.K. & Alitalo, K. (1997) Hyperplasia of lymphatic vessels in VEGF-C transgenic mice. *Science* **276**, 1423–1425.

Kajiya, K., Hirakawa, S., Ma, B., Drinnenberg, I. & Detmar, M. (2005) Hepatocyte growth factor promotes lymphatic vessel formation and function. *EMBO J.* **24**, 2885–2895.

Karkkainen, M.J., Haiko, P., Sainio, K., Partanen, J., Taipale, J., Petrova, T.V., Jeltsch, M., Jackson, D.G., Talikka, M., Rauvala, H., Betsholtz, C. & Alitalo, K. (2004) Vascular endothelial growth factor C is required for sprouting of the first lymphatic vessels from embryonic veins. *Nat. Immunol.* **5**, 74–80.

Karpanen, T. & Alitalo, K. (2008) Molecular biology and pathology of lymphangiogenesis. *Annu. Rev. Pathol.* **3**, 367–397.

Mishima, K., Watabe, T., Saito, A., Yoshimatsu, Y., Imaizumi, N., Masui, S., Hirashima, M., Morisada, T., Oike, Y., Araie, M., Niwa, H., Kubo, H., Suda, T. & Miyazono, K. (2007) Prox1 induces lymphatic endothelial differentiation via integrin α9 and other signaling cascades. *Mol. Biol. Cell* **18**, 1421–1429.

Morisada, T., Oike, Y., Yamada,Y., Urano, T., Akao, M., Kubota, Y., Maekawa, H., Kimura, Y., Ohmura, M., Miyamoto, T., Nozawa, S., Koh, G.Y., Alitalo, K. & Suda, T. (2005) Angiopoietin-1 promotes LYVE-1-positive lymphatic vessel formation. *Blood* **105**, 4649–4656.

Niwa, H., Miyazaki, J. & Smith, A.G. (2000) Quantitative expression of Oct-3/4 defines differentiation, dedifferentiation or self-renewal of ES cells. *Nat. Genet.* **24**, 372–376.

Oliver, G. (2004) Lymphatic vasculature development. *Nat. Rev. Immunol.* **4**, 35–45.

Park, J.I., Tsai, S.Y. & Tsai, M.J. (2003) Molecular mechanism of chicken ovalbumin upstream promoter-transcription factor (COUP-TF) actions. *Keio J. Med.* **52**, 174–181.

Petrova, T.V., Mäkinen, T., Mäkelä, T.P., Saarela, J., Virtanen, I., Ferrell, R.E., Finegold, D.N., Kerjaschki, D., Ylä-Herttuala, S. & Alitalo, K. (2002) Lymphatic endothelial reprogramming of vascular endothelial cells by the Prox-1 homeobox transcription factor. *EMBO J.* **21**, 4593–4599.

Qin, J., Gao, D.M., Jiang, Q.F., Zhou, Q., Kong, Y.Y., Wang, Y. & Xie, Y.H. (2004) Prospero-related homeobox (Prox1) is a corepressor of human liver receptor homolog-1 and suppresses the transcription of the cholesterol 7-α-hydroxylase gene. *Mol. Endocrinol.* **18**, 2424–2439.

Shin, J.W., Min, M., Larrieu-Lahargue, F., Canron, X., Kunstfeld, R., Nguyen, L., Henderson, J.E., Bikfalvi, A., Detmar, M. & Hong, Y.K. (2006) Prox1 promotes lineage-specific expression of fibroblast growth factor (FGF) receptor-3 in lymphatic endothelium: a role for FGF signaling in lymphangiogenesis. *Mol. Biol. Cell* **17**, 576–584.

Shirakihara, T., Saitoh, M. & Miyazono, K. (2007) Differential regulation of epithelial and mesenchymal markers by δEF1 proteins in epithelial mesenchymal transition induced by TGF-β. *Mol. Biol. Cell* **18**, 3533–3544.

Söderberg, O., Gullberg, M., Jarvius, M., Ridderstråle, K., Leuchowius, K.J., Jarvius, J., Wester, K., Hydbring, P., Bahram, F., Larsson, L.G. & Landegren, U. (2006) Direct observation of individual endogenous protein complexes *in situ* by proximity ligation. *Nat. Methods* **3**, 995–1000.

Söderberg, O., Leuchowius, K.J., Gullberg, M., Jarvius, M., Weibrecht, I., Larsson, L.G. & Landegren, U. (2008) Characterizing proteins and their interactions in cells and tissues using the *in situ* proximity ligation assay. *Methods* **45**, 227–232.

Srinivasan, R.S., Dillard, M.E., Lagutin, O.V., Lin, F.J., Tsai, S., Tsai, M.J., Samokhvalov, I.M. & Oliver, G. (2007) Lineage tracing demonstrates the venous origin of the mammalian lymphatic vasculature. *Genes Dev.* **21**, 2422–2432.

Steffensen, K.R., Holter, E., Båvner, A., Nilsson, M., Pelto-Huikko, M., Tomarev, S. & Treuter, E. (2004) Functional conservation of interactions between a homeodomain cofactor and a mammalian FTZ-F1 homologue. *EMBO Rep.* **5**, 613–619.

Veikkola, T., Jussila, L., Makinen, T., Karpanen, T., Jeltsch, M., Petrova, T.V., Kubo, H., Thurston, G., McDonald, D.M., Achen, M.G., Stacker, S.A. & Alitalo, K. (2001) Signalling via vascular endothelial growth factor receptor-3 is sufficient for lymphangiogenesis in transgenic mice. *EMBO J.* **20**, 1223–1231.

Vlahakis, N.E., Young, B.A., Atakilit, A. & Sheppard, D. (2005) The lymphangiogenic vascular endothelial growth factors VEGF-C and -D are ligands for the integrin α9β1. *J. Biol. Chem.* **280**, 4544–4552.

Watabe, T., Nishihara, A., Mishima, K., Yamashita, J., Shimizu, K., Miyazawa, K., Nishikawa, S. & Miyazono, K. (2003) TGF-β receptor kinase inhibitor enhances growth and integrity of embryonic stem cell-derived endothelial cells. *J. Cell Biol.* **163**, 1303–1311.

Wigle, J.T., Harvey, N., Detmar, M., Lagutina, I., Grosveld, G., Gunn, M.D., Jackson, D.G. & Oliver, G. (2002) An essential role for Prox1 in the induction of the lymphatic endothelial cell phenotype. *EMBO J.* **21**, 1505–1513.

Wigle, J.T. & Oliver, G. (1999) Prox1 function is required for the development of the murine lymphatic system. *Cell* **98**, 769–778.

You, L.R., Lin, F.J., Lee, C.T., DeMayo, F.J., Tsai, M.J. & Tsai, S.Y. (2005) Suppression of Notch signalling by the COUP-TFII transcription factor regulates vein identity. *Nature* **435**, 98–104.

Received: 7 September 2008
Accepted: 6 December 2008

Supporting Information/Supplementary material

The following Supporting Information can be found in the online version of the article:

Figure S1 Efficacy of knockdown of COUP-TFII expression in HUVECs.

Figure S2 COUP-TFII suppresses Prox1-induced cyclin E2 expression in HUVECs.

Figure S3 Interaction of endogenous Prox1 and COUP-TFII in HDLECs.

Figure S4 Endogenous level of COUP-TFII expression plays important roles in the maintenance of characteristics of HDLECs.

Table S1 Primers used for RT-PCR

Additional Supporting Information may be found in the online version of the article.

Please note: Wiley-Blackwell are not responsible for the content or functionality of any supporting information supplied by the authors. Any queries (other than missing material) should be directed to the corresponding author for the article.

Identification of targets of Prox1 during in vitro vascular differentiation from embryonic stem cells: functional roles of HoxD8 in lymphangiogenesis

Kaori Harada[1], Tomoko Yamazaki[1], Caname Iwata[1], Yasuhiro Yoshimatsu[1], Hitoshi Sase[1], Koichi Mishima[1], Yasuyuki Morishita[1], Masanori Hirashima[2], Yuichi Oike[3], Toshio Suda[4], Naoyuki Miura[5], Tetsuro Watabe[1,*] and Kohei Miyazono[1]

[1]Department of Molecular Pathology, Graduate School of Medicine, University of Tokyo, Tokyo 113-0033, Japan
[2]Division of Vascular Biology, Department of Physiology and Cell Biology, Kobe University Graduate School of Medicine, Kobe 650-0017, Japan
[3]Department of Molecular Genetics, Graduate School of Medical Sciences, Kumamoto University, Kumamoto 860-0811, Japan
[4]Department of Cell Differentiation, The Sakaguchi Laboratory, School of Medicine, Keio University, Tokyo 160-8582, Japan
[5]Department of Biochemistry, Hamamatsu University School of Medicine, Hamamatsu 431-3192, Japan
*Author for correspondence (t-watabe@umin.ac.jp)

Accepted 21 August 2009
Journal of Cell Science 122, 3923-3930 Published by The Company of Biologists 2009
doi:10.1242/jcs.052324

Summary

During lymphatic development, Prox1 plays central roles in the differentiation of blood vascular endothelial cells (BECs) into lymphatic endothelial cells (LECs), and subsequently in the maturation and maintenance of lymphatic vessels. However, the molecular mechanisms by which Prox1 elicits these functions remain to be elucidated. Here, we identified FoxC2 and angiopoietin-2 (Ang2), which play important roles in the maturation of lymphatic vessels, as novel targets of Prox1 in mouse embryonic-stem-cell-derived endothelial cells (MESECs). Furthermore, we found that expression of HoxD8 was significantly induced by Prox1 in MESECs, a finding confirmed in human umbilical vein endothelial cells (HUVECs) and human dermal LECs (HDLECs). In mouse embryos, HoxD8 expression was significantly higher in LECs than in BECs. In a model of inflammatory lymphangiogenesis, diameters of lymphatic vessels of the diaphragm were increased by adenovirally transduced HoxD8. We also found that HoxD8 induces Ang2 expression in HDLECs and HUVECs. Moreover, we found that HoxD8 induces Prox1 expression in HUVECs and that knockdown of HoxD8 reduces this expression in HDLECs, suggesting that Prox1 expression in LECs is maintained by HoxD8. These findings indicate that transcriptional networks of Prox1 and HoxD8 play important roles in the maturation and maintenance of lymphatic vessels.

Supplementary material available online at
http://jcs.biologists.org/cgi/content/full/122/21/3923/DC1

Key words: HoxD8, Prox1, Lymphangiogenesis, Angiopoietin-2

Introduction

The lymphatic system plays very important roles in the maintenance of tissue-fluid homeostasis and mediation of the afferent immune response (Karpanen and Alitalo, 2008). Insufficiency or obstruction of function of this system results in lymphedema, characterized by leaking of tissue fluid and swelling of affected tissue. Furthermore, in many types of cancer, the lymphatic vessels provide a major pathway for tumor metastasis to lymph nodes. Understanding of the molecular mechanisms that govern the formation of the lymphatic system is thus of crucial importance.

Embryonic lymphatic endothelial cells (LECs) arise by sprouting from the jugular veins and migrate towards mesenchymal cells expressing vascular endothelial growth factor (VEGF)-C, leading to the formation of the primary lymphatic plexus (Oliver, 2004). During these processes, the prospero-related homeobox-1 (Prox1) transcription factor marks the first LECs within embryonic cardinal veins. Importantly, in Prox1-deficient mice, the migration of endothelial cells expected to express Prox1 towards VEGF-C is arrested, resulting in complete lack of the lymphatic vasculature and embryonic lethality (Wigle and Oliver, 1999; Wigle et al., 2002). Transcription-profiling analyses have shown that Prox1 induces the expression of various LEC markers – including VEGFR3, a receptor for VEGF-C – in human dermal microvascular endothelial cells (HDMECs) (Hong et al., 2002; Petrova et al., 2002). Recently, we also showed that Prox1 inhibits sheet formation of mouse embryonic stem (ES)-cell-derived endothelial cells (MESECs) and induced various LEC markers, such as integrin α9 (Mishima et al., 2007). Furthermore, we confirmed that Prox1 induces integrin-α9 expression in human umbilical vein endothelial cells (HUVECs) and human dermal LECs (HDLECs), and found that integrin α9 is required for Prox1-induced inhibition of sheet formation and promotion of migration towards VEGF-C. Interestingly, Prox1 also downregulates the expression of blood vascular endothelial cell (BEC) markers such as VEGFR2 (Petrova et al., 2002; Mishima et al., 2007), suggesting that Prox1 regulates the differentiation of embryonic BECs to LECs by reprogramming gene expression profiles.

The primary lymphatic plexus, which is composed of thin lymphatic vessels, undergoes enlargement and maturation to form collecting lymphatic vessels that have characteristics different from those of primary lymphatic vessels, such as valve formation and attachment of smooth-muscle cells. FoxC2 transcription factor and angiopoietin-2 (Ang2), a ligand for Tie2 receptor tyrosine kinase, have been implicated in these maturation processes (Gale et al.,

2002; Dellinger et al., 2008; Petrova et al., 2004). Prox1 expression is maintained in mature LECs, and is required for maintenance of the expression of LEC markers and characteristics of LECs (Mishima et al., 2007; Srinivasan et al., 2007; Johnson et al., 2008). However, the molecular mechanisms by which Prox1 regulates the maturation of lymphatic vessels remain to be elucidated.

In the present study, we identified novel target genes of Prox1 in MESECs. Expression of FoxC2 and Ang2 was induced by Prox1. Furthermore, we found that Prox1 induces the expression of HoxD8, which is capable of increasing the caliber of lymphatic vessels in an in vivo model of inflammatory lymphangiogenesis. These findings suggest that Prox1 induces the expression of a distinct group of genes to promote the maturation of lymphatic vessels.

Results

Identification of Prox1 targets in mouse ES-cell-derived endothelial cells

We previously showed that *Prox1* transgene expression in MESECs induces the expression of a group of genes that induce the differentiation of BECs to LECs (Mishima et al., 2007). To further identify the Prox1 target genes that are involved in lymphatic development, we performed cDNA microarray analysis using endothelial cells derived from mouse ES cells carrying a tetracycline (Tc)-inducible *Prox1* transgene. Among approximately 400 genes whose levels of expression were regulated by Prox1 (supplementary material Tables S1 and S2), we found that expression of integrin α9, cyclin E1 and fibroblast growth factor receptor 3 (FGFR3), all of which have been reported to be Prox1 targets (Mishima et al., 2007; Petrova et al., 2002; Shin et al., 2006), was induced by Prox1 (Table 1). These findings suggest that cDNA microarray analysis identified an appropriate set of Prox1 targets.

Prox1 induces the expression of Ang2 and FoxC2

Among the candidate molecules of Prox1 targets identified by the cDNA microarray analysis, we next searched for factors that have been implicated in lymphatic formation. Although Ang2 and FoxC2 have been implicated in the maturation of lymphatic vessels (Gale et al., 2002; Dellinger et al., 2008; Petrova et al., 2004), the molecular mechanisms by which their expression is regulated in LECs have not yet been elucidated. Because we found that their expression was induced by Prox1, we first confirmed the effects of Prox1 on the expression of Ang2 and FoxC2 in MESECs by quantitative reverse transcriptase (RT)-PCR analysis. As previously reported (Mishima et al., 2007), the removal of Tc from culture of VEGFR2-expressing (VEGFR2+) cells derived from Tc-Prox1 ES cells induced *Prox1* transgene expression, whereas that from Tc-Empty ES cells did not (Fig. 1A,E). As shown in Fig. 1B,C, *Prox1* transgene expression significantly promoted the expression of Ang2 and FoxC2.

We next examined whether these effects of Prox1 are observed in other types of endothelial cells. HUVECs were infected with adenovirus encoding Prox1 (Ad-Prox1) or non-coding adenoviruses (Ad-Null) (Fig. 2Aa,E). When *Prox1* was transduced into HUVECs, Ang2 expression was significantly induced (Fig. 2Ba,E). By contrast, FoxC2 expression was only mildly induced (Fig. 2Ca,E).

Because LECs, but not BECs, express Prox1 endogenously (Fig. 2Ab,E), we expected that the levels of expression of endogenous Ang2 and FoxC2 might be higher in HDLECs than in HUVECs. As shown in Fig. 2Bb and E, Ang2 expression was higher in HDLECs than in HUVECs. However, the levels of expression of *FoxC2* mRNA were comparable in HDLECs and HUVECs, and the expression of FoxC2 protein was only slightly higher in HDLECs than in HUVECs (Fig. 2Cb,E).

We previously showed that endogenous Prox1 expression in HDLECs is required for maintenance of the expression of LEC markers, including VEGFR3 and integrin α9 (Mishima et al., 2007).

Table 1. Examples of genes that are upregulated by Prox1

Category	Gene symbol	Gene name
Transcription factors	*Foxc1*	Forkhead box C1
	Foxc2	Forkhead box C2
	Foxp1	Forkhead box P1
	Hoxd8	Homeobox D8
	Hoxd9	Homeobox D9
	Id1	Inhibitor of DNA binding 1
	Id2	Inhibitor of DNA binding 2
	Id3	Inhibitor of DNA binding 3
	Id4	Inhibitor of DNA binding 4
	Irx3	Iroquois related homeobox 3
	Irx5	Iroquois related homeobox 5
	Klf4	Kruppel-like factor 4
	Snai1	Snail homolog 1
Adhesion molecules	*Itga8*	Integrin alpha 8
	Itga9	Integrin alpha 9
Growth factors	*Angpt2*	Angiopoietin 2
	Fgf13	Fibroblast growth factor 13
	Igf1	Insulin-like growth factor 1
Cytokines and chemokines	*Cxcl12*	Chemokine (C-X-C motif) ligand 12
Cell-cycle control	*Aurka*	Aurora kinase A
	Aurkb	Aurora kinase B
	Ccna2	Cyclin A2
	Ccnb1	Cyclin B1
	Ccne1	Cyclin E1
	Ccnf	Cyclin F
	Plk4	Polo-like kinase 4
	Sgol1	Shugoshin-like 1
	Skp2	S-phase kinase-associated protein 2 (p45)
Receptors	*Acvr2b*	Activin receptor IIB
	Fgfr3	Fibroblast growth factor receptor 3
	Pdgfra	Platelet derived growth factor, alpha polypeptide
	Lifr	Leukemia inhibitory factor receptor
	Tnfrsf19	Tumor necrosis factor receptor superfamily, member 19
Other	*Fst*	Follistatin
	Hmgb3	High mobility group box 3
	Jag1	Jagged 1
	Plce1	Phospholipase C, epsilon 1
	Prkcm	Protein kinase C, mu
	Prom1	Prominin 1, CD133
	Racgap1	Rac GTPase-activating protein 1
	Thbs4	Thrombospondin 4

To identify genes whose expression was increased by Prox1 in MESECs, three criteria were applied to 45102 genes in the GeneChip Mouse Genome 430 2.0 Array. (1) Signal intensities in Tc-Prox1/Tc– (MESECs expressing the *Prox1* transgene) were >36, and given 'present' calls. (2) Signals were increased by Prox1 more than twofold compared with control Tc-Prox1/Tc+ (MESECs not expressing the *Prox1* transgene). (3) Signals were not increased in Tc-Empty/Tc– compared with Tc-Empty/Tc+ (in order to remove genes whose expression is altered by Tc); 310 genes met these restrictions, some of which are listed here. Complete lists of genes regulated by Prox1 are included in supplementary material Tables S1 and S2.

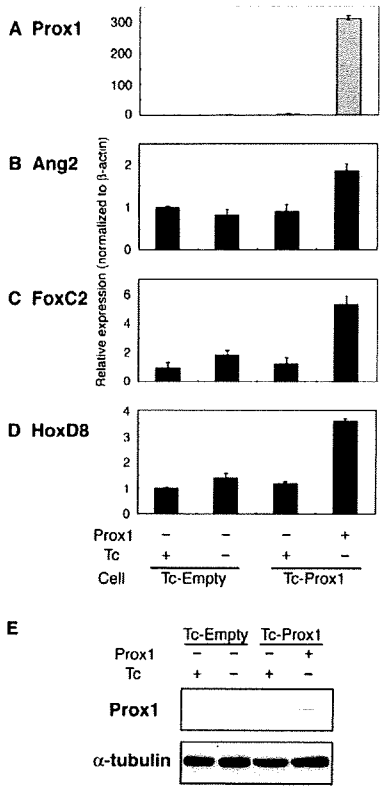

Fig. 1. Identification of Prox1 targets in MESECs. (A-D) Effects of the *Prox1* transgene (A; light grey bar) on expression of Ang2 (B), FoxC2 (C) and HoxD8 (D) were examined in MESECs by quantitative RT-PCR analyses. VEGFR2-expressing endothelial progenitor cells were sorted from differentiated ES cells carrying a tetracycline (Tc)-regulated transgene encoding mouse Prox1 (Tc-Prox1) or no transgene (Tc-Empty), and re-differentiated in the presence (+) or absence (–) of Tc. Expression of *Prox1* transgene was induced in the absence of Tc in Tc-Prox1 cells (A). Bars, s.d. (E) Levels of Prox1 (upper panel) and α-tubulin (lower panel; internal control) proteins were examined by immunoblotting.

To examine the roles of endogenous Prox1 in HDLECs, HDLECs were transfected with siRNAs for *Prox1* (siProx1) or negative control siRNA (siNC). When Prox1 expression was knocked-down (Fig. 2Ac,E), the expression levels of *Ang2* and *FoxC2* mRNAs were not significantly altered, and those of Ang2 and FoxC2 proteins were only weakly repressed (Fig. 2Bc,Cc,E). These results suggest that Prox1 is able to induce the expression of Ang2 in embryonic and mature endothelial cells, and that Prox1 differentially induces FoxC2 expression in embryonic and mature endothelial cells.

HoxD8 is a novel target of Prox1 in LECs

To identify novel targets of Prox1 involved in lymphangiogenesis, we focused on transcription factors whose expression was upregulated by Prox1 in MESECs. In addition to FoxC2, we identified homeobox transcription factors including HoxD8 and HoxD9 (Table 1). Homeobox (Hox) genes encode transcription factors, which play crucial roles in cell proliferation, migration and differentiation (Pearson et al., 2005). Hox proteins bind DNA weakly, but gain specificity and affinity by interaction with other proteins, termed modulators or cofactors. We therefore examined whether HoxD8 and/or HoxD9 form transcription complexes and function in a lymphatic-vessel-specific fashion. Some Hox-family members, such as HoxA9 and HoxD3, have been implicated in development of the cardiovascular system and endothelial-cell activation during neovascularization (Bruhl et al., 2004; Boudreau et al., 2004). However, the roles of HoxD8 in the vascular system have not yet been reported. Furthermore, no Hox-family members have yet been implicated in lymphangiogenesis.

Induction of HoxD8 expression by Prox1 in MESECs was confirmed by quantitative RT-PCR analysis (Fig. 1D). We also found that Prox1 induces HoxD8 expression in HUVECs (Fig. 2Da), suggesting that HoxD8 is induced by Prox1 in various types of endothelial cell.

We next examined the expression of HoxD8 in LECs. As shown in Fig. 2Db, the level of expression of HoxD8 in HDLECs was higher than that in HUVECs. Furthermore, knockdown of Prox1 expression in HDLECs led to a decrease in HoxD8 expression (Fig. 2Dc). These results suggest that the amount of *HoxD8* transcripts is increased during Prox1-induced differentiation of BECs into LECs and that this increased expression is maintained by Prox1 in LECs, although these results were not confirmed at protein level because of the lack of antibodies that are able to detect endogenous HoxD8 proteins.

Among paralogous group-8 Hox genes, *HoxD8* alone is expressed in LECs

HoxD8 is one of the paralogous group-8 Hox genes; this group also includes *HoxB8* and *HoxC8*. HoxD8-mutant mice exhibited two anterior homeotic transformations of thoracic vertebrae, although both of these phenotypes exhibited very low penetrance (van den Akker et al., 2001). Phenotypes of double and triple mutants revealed that HoxB8, HoxC8 and HoxD8 have redundant functions at the upper thoracic and sacral levels, including positioning of the hindlimbs. To examine whether other group-8 Hox genes are involved in lymphangiogenesis, we determined the expression of *HoxB8*, *HoxC8* and *HoxD8* in HUVECs and HDLECs by conventional RT-PCR analysis. Whereas all paralogous group-8 Hox genes were expressed in HUVECs, only *HoxD8* was expressed in HDLECs (Fig. 3A). Furthermore, Prox1 failed to induce the expression of HoxB8 and HoxC8 in HUVECs (Fig. 3B), whereas it induced HoxD8 expression (Fig. 2Da), suggesting important functions for HoxD8 among the paralogous group-8 Hox genes in LECs.

HoxD8 is expressed in LECs of mouse embryos

Previous studies showed that HoxD8 is expressed along the anteroposterior axis in the nervous system, vertebral column, gut and kidney at the posterior end of the embryo, and that expression of it extends anteriorly (Izpisùa-Belmonte et al., 1990; van den Akker et al., 2001). However, expression of it in the developing lymphatic vessels has not been reported. To examine the in vivo significance of our finding that Prox1 induces HoxD8 expression in various cultured endothelial cells, we determined the levels of expression of HoxD8 in BECs and LECs derived from mouse embryos. BECs and LECs were isolated from embryonic day 14.5 (E14.5) mouse embryos by fluorescence-activated cell sorting (FACS) using antibodies for CD31 and LYVE-1, respectively, as described in Materials and Methods (Hirashima et al., 2008). The level of expression of HoxD8 in LECs was significantly higher than that in BECs (Fig. 4). This result suggests that the in vitro induction

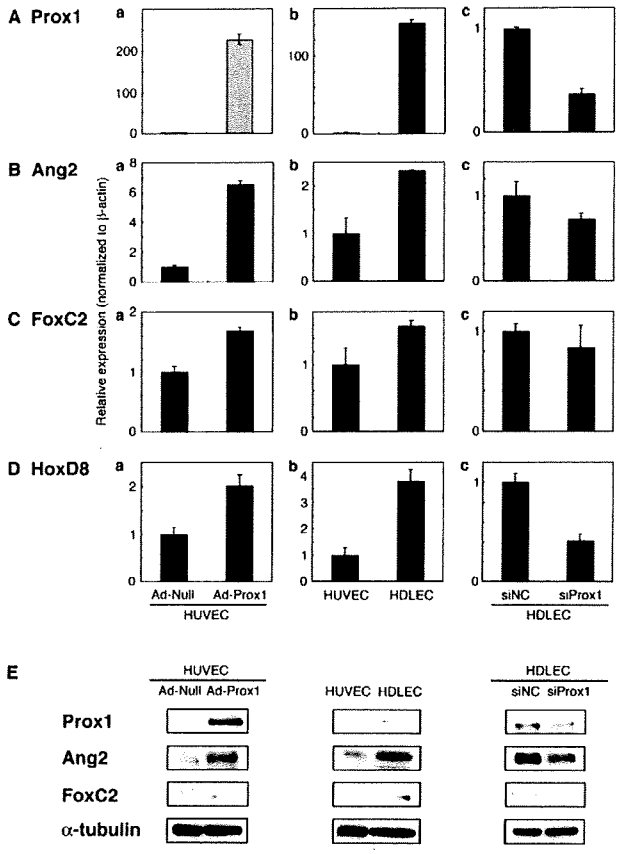

Fig. 2. Roles of Prox1 in the expression of its targets in BECs and LECs. (Aa-Da) Effect of gain-of-function of Prox1 via the *Prox1* transgene (A; light grey bar) on the endogenous expression of Ang2 (B), FoxC2 (C) and HoxD8 (D). HUVECs were infected with adenovirus encoding Prox1 (Ad-Prox1) or non-coding adenovirus (Ad-Null), followed by quantitative RT-PCR analyses. (Ab-Db) Expression of endogenous Prox1 (A; dark grey bar), Ang2 (B), FoxC2 (C) and HoxD8 (D) was examined in native HUVECs and HDLECs. (Ac-Dc) Effect of loss-of-function of Prox1 (A) on the expression of Ang2 (B), FoxC2 (C) and HoxD8 (D). HDLECs were transfected with siRNA for *Prox1* (siProx1) or negative control siRNA (siNC), followed by quantitative RT-PCR analyses. Bars, s.d. (E) Levels of Prox1, Ang2, FoxC2 and α-tubulin (internal control) proteins were examined by immunoblotting.

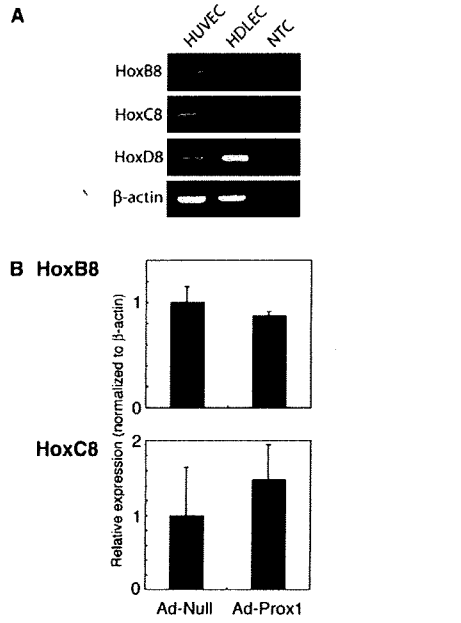

Fig. 3. Expression of paralogous group-8 Hox genes in BECs and LECs. (A) Expression of HoxB8, HoxC8 and HoxD8 in HUVECs and HDLECs was examined by conventional RT-PCR analysis. β-actin was used as an internal control. NTC, no template control. (B) Effect of the *Prox1* transgene on the expression of HoxB8 (top) and HoxC8 (bottom). HUVECs were infected with adenovirus encoding Prox1 (Ad-Prox1) or non-coding adenovirus (Ad-Null), followed by quantitative RT-PCR analyses. Bars, s.d.

of HoxD8 expression by Prox1 demonstrated in the present study might mimic the process of embryonic lymphatic development.

HoxD8 increases the diameters of lymphatic vessels in an in vivo mouse model of inflammatory lymphangiogenesis

To examine the roles of HoxD8 in lymphangiogenesis, we used a mouse model of chronic inflammation (Iwata et al., 2007). In this model, chronic aseptic peritonitis was induced by repeated intraperitoneal injection of thioglycollate medium, a proinflammatory agent, into immunocompetent BALB/c mice. As shown in Fig. 5A, outgrowths of lymphatic vessels were detected by anti-LYVE-1 staining in the inflammatory plaques formed on the peritoneal surface of the diaphragm. When adenoviruses encoding β-galactosidase (*lacZ*) were injected intraperitoneally in combination with thioglycollate medium, these lymphatic vessels were stained for anti-β-galactosidase (Fig. 5A), suggesting that newly generated lymphatic vessels are transduced by adenoviruses.

When adenoviruses encoding HoxD8 were injected, the diameters of lymphatic vessels increased significantly compared with those injected with adenoviruses encoding β-galactosidase (Fig. 5B,C). These findings suggest that HoxD8 regulates the caliber of lymphatic vessels.

The inflammatory plaques formed on the surface of the diaphragm consist of macrophages that express VEGF-A, VEGF-C and VEGF-D (Iwata et al., 2007). To examine whether HoxD8 that was transduced into macrophages alters the expression of angiogenic and/or lymphangiogenic factors, we determined the levels of expression of VEGF-A, VEGF-C and VEGF-D in the plaques that mainly consisted of macrophages. As shown in Fig. 5D, levels of expression were not statistically changed by adenovirally transduced *HoxD8*. These results suggest that the effects of HoxD8 on the lymphatic vessels are not indirectly mediated through VEGF-A, VEGF-C or VEGF-D secreted from macrophages.

HoxD8 induces the expression of Ang2

Tie2 receptor tyrosine kinase is activated by its ligand, Ang1, and transduces signals to induce maturation of blood and lymphatic vessels. Ang2 is considered as an antagonist or agonist for Tie2, depending on endothelial-cell status. Furthermore, lymphatic phenotypes in knockout mice deficient for Ang2 were rescued by knocking-in the *Ang1* gene in the *Ang2* locus (Gale et al., 2002), suggesting that Ang2 might function as an agonist for Tie2 to induce

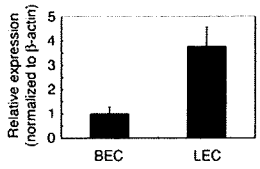

Fig. 4. Expression of HoxD8 in BECs and LECs derived from mouse embryos. E14.5 mouse embryos were dissociated, followed by FACS sorting with anti-CD45, -LYVE-1 and -CD31 antibodies, as described in Materials and Methods (Hirashima et al., 2008). Equivalent amount of total RNAs prepared from CD45− CD31+ LYVE-1− BEC fractions (1.5% in CD45− cells) and CD45− CD31− LYVE-1+ LEC fractions (0.2% in CD45− cells) were subjected to quantitative RT-PCR analysis of transcripts for HoxD8. Bars, s.d.

maturation of lymphatic vessels. To examine the relationship between HoxD8 and Ang2, both of which are targets of Prox1, we examined the level of expression of Ang2 in HDLECs transfected with siRNAs for *HoxD8* (siHoxD8) or siNC (Fig. 6A). A decrease in HoxD8 expression (Fig. 6A, top) resulted in partial decrease in the amounts of transcripts (Fig. 6A, bottom) and proteins (Fig. 6B) of Ang2 in HDLECs.

We next examined the effects of gain-of-function of HoxD8 on Ang2 expression in HUVECs. When *HoxD8* as well as *Prox1* was transduced into HUVECs, the level of *Ang2* transcripts was increased (Fig. 6C), which was confirmed at protein level (Fig. 6D). These results suggest that both Prox1 and HoxD8, one of the targets of Prox1, induce Ang2 expression.

HoxD8 maintains Prox1 expression in LECs

Although Prox1 expression is maintained in mature LECs, the molecular mechanisms by which it is maintained have not yet been elucidated. We therefore examined whether HoxD8, the expression of which is induced by Prox1, plays any roles in the regulation of Prox1 expression. When HoxD8 expression in HDLECs was knocked-down by siRNA (Fig. 6A, top), endogenous expression of Prox1 decreased (Fig. 7A), suggesting that HoxD8 is required for the maintenance of endogenous Prox1 expression in LECs. Moreover, we found that the expression of a *HoxD8* transgene (Fig. 7B, top) induced endogenous Prox1 expression in HUVECs (Fig. 7B, bottom). These results were confirmed at the protein level by western blot analysis (Fig. 7C). Taken together, these findings suggest that HoxD8 plays an important role in positive feedback of Prox1 expression in LECs.

Discussion

In the present study, we identified a novel group of Prox1 targets using cDNA microarray analysis of MESECs. We found that Prox1 induces the expression of Ang2 and FoxC2, both of which are involved in the maturation of lymphatic vessels (Gale et al., 2002; Dellinger et al., 2008; Petrova et al., 2004). We also found that Prox1 induces the expression of HoxD8, which increased the diameter of lymphatic vessels in an in vivo model of inflammatory lymphangiogenesis. Furthermore, HoxD8 maintains endogenous Prox1 expression in LECs.

Although previous studies (Petrova et al., 2002; Hong et al., 2002; Shin et al., 2006) identified various LEC markers as Prox1 targets using microarray analyses of mature endothelial cells (HDMECs), they did not find that Ang2 or FoxC2 expression was upregulated

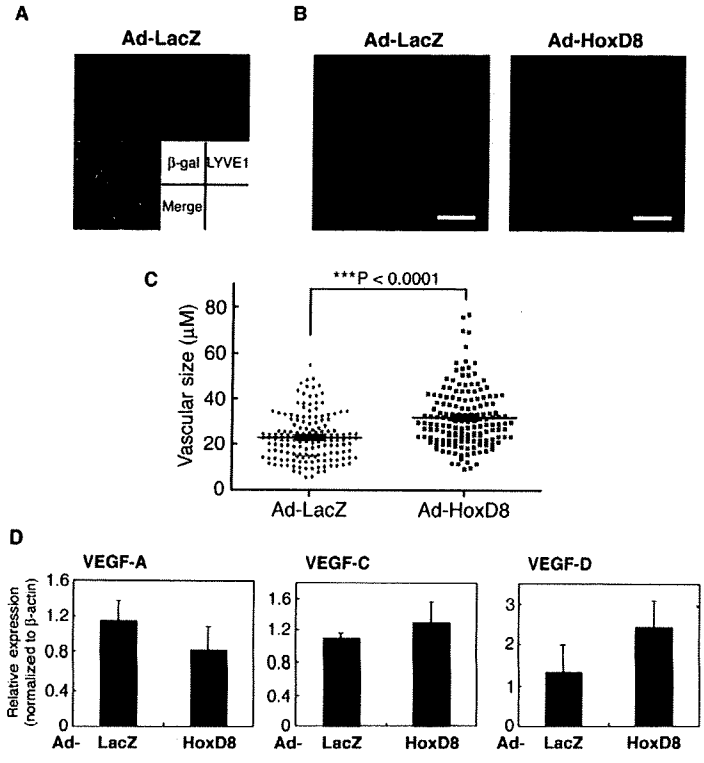

Fig. 5. Effects of HoxD8 on lymphangiogenesis in a mouse model of chronic aseptic peritonitis. (A) Repeated intraperitoneal injection of thioglycollate medium in combination with adenoviruses encoding β-galactosidase resulted in the formation of inflammatory plaques on the peritoneal surface of the diaphragm. Whole-mount staining with anti-LYVE-1 (red) and anti-β-galactosidase (green) is shown. (B) Adenoviruses encoding β-galactosidase or HoxD8 were injected in combination with thioglycollate medium, followed by immunostaining for LYVE-1. Scale bars: 200 μm. (C) Diameters of lymphatic vessels in plaques were quantified. Points represent individual values and long bars represent mean of the diameters of LYVE-1-positive vessels. Short bars, s.e. (150 vessels from three mice were examined); ***$P<0.0001$. (D) Effects of HoxD8 on expression of angiogenic and/or lymphangiogenic factors in plaques. Plaques that mainly consist of macrophages were obtained from the peritoneal surface of the diaphragm, followed by quantitative RT-PCR analyses for VEGF-A, VEGF-C and VEGF-D. Bars, s.e.; $P>0.05$.

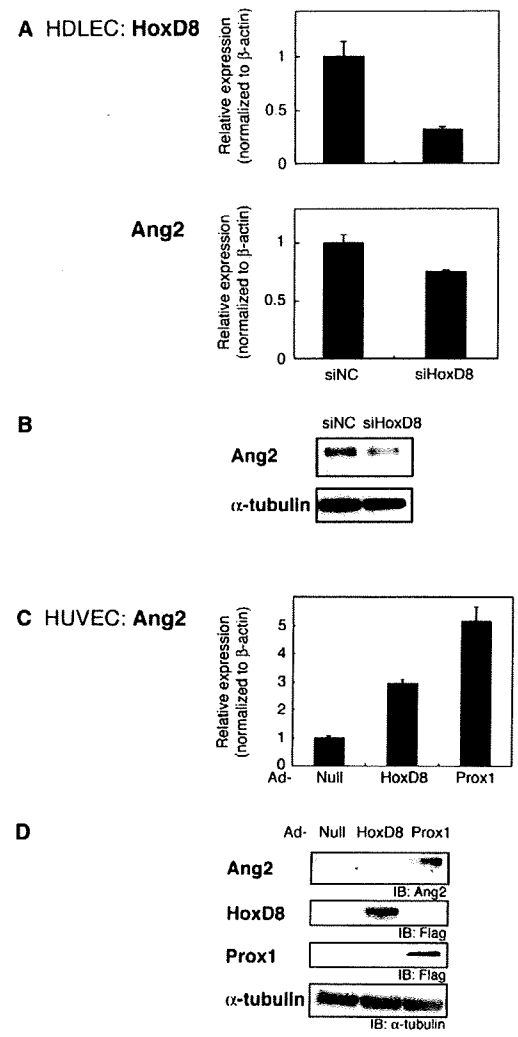

Fig. 6. Effects of HoxD8 on Ang2 expression in LECs and BECs. (A) Effect of loss-of-function of HoxD8 on expression of Ang2 in LECs. HDLECs were transfected with siRNA for *HoxD8* (siHoxD8) or negative control siRNA (siNC), followed by quantitative RT-PCR analyses for HoxD8 (top) and Ang2 (bottom). (B) Levels of Ang2 (top) and α-tubulin (bottom; internal control) proteins were examined by immunoblotting. (C) Effect of gain-of-function of HoxD8 and Prox1 on expression of Ang2. HUVECs were infected with adenovirus encoding HoxD8 (Ad-HoxD8) or Prox1 (Ad-Prox1), or non-coding adenovirus (Ad-Null), followed by quantitative RT-PCR analyses for Ang2. Bars, s.d. (D) Protein levels of endogenous Ang2 and α-tubulin (internal control) were examined by immunoblotting (IB). Expression of adenovirally introduced FLAG-tagged HoxD8 and Prox1 proteins was confirmed by immunoblotting (IB) using an anti-FLAG antibody.

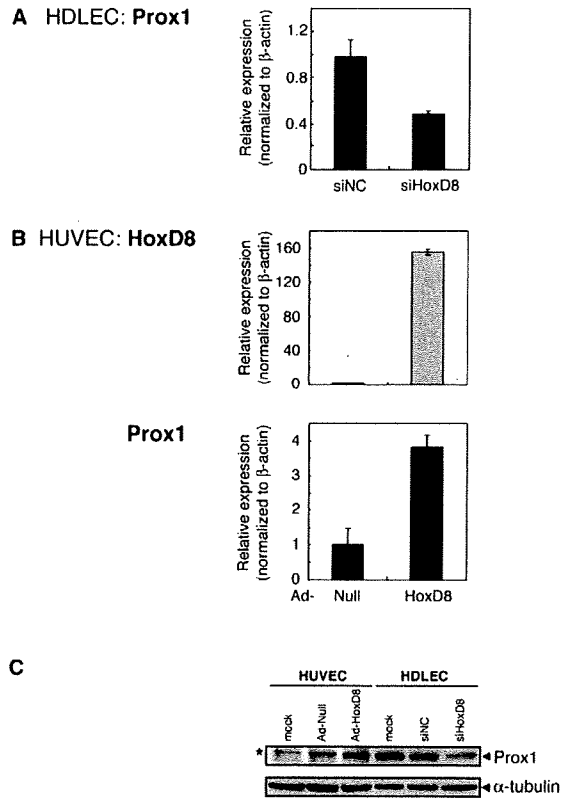

Fig. 7. Effects of HoxD8 on Prox1 expression in LECs and BECs. (A) Effect of loss-of-function of HoxD8 on the expression of Prox1 in LECs. HDLECs were transfected with siRNA for HoxD8 (siHoxD8) or negative control siRNA (siNC), followed by quantitative RT-PCR analyses for Prox1. (B) Effect of gain-of-function of HoxD8 on expression of Prox1. HUVECs were infected with adenovirus encoding HoxD8 (Ad-HoxD8) or non-coding adenovirus (Ad-Null), followed by quantitative RT-PCR analyses for HoxD8 transgene (top; light grey) and endogenous Prox1 (bottom). Bars, s.d. (C) Expression of endogenous Prox1 protein in HUVECs and HDLECs is shown by western blotting. Asterisk represents non-specific bands.

by Prox1. As shown in Fig. 2Ca, induction of FoxC2 by Prox1 in HUVECs was not as potent as that in MESECs (Fig. 1C), which might explain why previous studies did not identify these genes as targets of Prox1. By contrast, VEGFR3 expression was not upregulated by Prox1 in our analysis. VEGFR3 expression has been reported to be high in embryonic endothelial cells (Tammela et al., 2008), which might have led to the failure of VEGFR3 induction by Prox1 in MESECs. These results suggest that MESECs might represent a different status of endothelial cells from HDMECs and HUVECs, and confirm the usefulness of the cDNA microarray analysis performed in the present study.

Ablation of Ang2 or FoxC2 does not result in defects in the formation of the primary lymphatic plexus, which is severely affected in Prox1-knockout mice (Wigle and Oliver, 1999). However, remodeling and maturation of lymphatic vessels is defective in mice deficient for Ang2 or FoxC2 (Gale et al., 2002; Dellinger et al., 2008; Petrova et al., 2004). In Ang2-deficient mice, lymphatic vessels do not mature or they exhibit a collecting vessel phenotype, without proper recruitment of smooth-muscle cells or postnatal remodeling (Dellinger et al., 2008). FoxC2-knockout mice exhibit abnormal lymphatic vascular patterning, increased pericyte recruitment of lymphatic vessels and defective valve formation (Petrova et al., 2004), which lead to the phenotype of lymphedema-distichiasis syndrome (LD). The present finding that Prox1 induces the expression of Ang2 and FoxC2 suggests

that Prox1 indirectly induces the maturation of embryonic lymphatic vessels through induction of a group of maturation-inducing factors.

We identified HoxD8 as a novel target of Prox1. Hox genes play very important roles during embryonic development. We found that HoxD8 increases the caliber of lymphatic vessels in a model of inflammatory lymphangiogenesis. However, this effect of HoxD8 on the caliber size did not mimic the functions of Prox1. We found that adenoviruses encoding Prox1 significantly decreased the diameters of lymphatic vessels (supplementary material Fig. S1A,B) and that Prox1 seemed to increase the number of lymphatic vessels as compared with the control (supplementary material Fig. S1A). Both Prox1 and HoxD8 induced the expression of Ang2, which is involved in the remodeling and maturation of lymphatic vessels. Similar to Prox1, however, adenoviruses encoding Ang2 significantly decreased the diameters of lymphatic vessels (supplementary material Fig. S1C,D), suggesting that Ang2 is not involved in the HoxD8-mediated increase of the caliber of lymphatic vessels. Several lines of evidence have suggested that Ang2 that is present in smooth-muscle cells plays important roles in the formation of lymphatic systems (Gale et al., 2002; Dellinger et al., 2008). The effects of adenovirally introduced Ang2 on the lymphatic formation (supplementary material Fig. S1C,D) might mimic the effects caused by Ang2 secreted by smooth-muscle cells.

Furthermore, studies using in-vitro-cultured HDLECs revealed that the decrease in HoxD8 expression failed to affect the number of HDLECs (supplementary material Fig. S2A). We also found that the decreased HoxD8 expression did not alter the migration of HDLECs towards VEGF-C (supplementary material Fig. S2B). Nonetheless, adenovirally introduced HoxD8 might have caused inflammatory cells to secrete a different profile of lymphangiogenic factors. Although we showed that HoxD8 does not significantly alter the expression of VEGF-A, VEGF-C or VEGF-D in macrophages (Fig. 5D), it might have induced the expression of other cytokines that regulate the caliber size of lymphatic vessels. The molecular mechanisms by which HoxD8 regulates the diameter of lymphatic vessels remain to be elucidated in the future.

We found that both Prox1 and HoxD8 induce Ang2 expression. During angiogenesis, FoxC2 controls Ang2 expression by direct activation of the Ang2 promoter and promotes maturation of blood vessels (Xue et al., 2008). Taken together with the present finding that Prox1 induces the expression of FoxC2 and HoxD8, these results suggest that the transcriptional networks that include Prox1, HoxD8 and FoxC2 play important roles in Ang2 expression during lymphatic development.

Recently, Sox18 was reported to play important roles in the initial induction of Prox1 expression in venous endothelial cells by direct binding to the *Prox1* promoter (François et al., 2008). Sox18 is expressed in a subset of venous endothelial cells prior to Prox1 expression and is coexpressed with Prox1 during the formation of the primary lymphatic plexus. However, Sox18 expression in LECs ceases during the maturation of lymphatic vessels. Endogenous Prox1 expression in LECs thus requires transcriptional inducers that are expressed in LECs. In the present study, we found that HoxD8 maintains endogenous Prox1 expression in LECs. These results suggest a novel positive-feedback-loop mechanism in which Prox1 expression is maintained by HoxD8, the expression of which is induced by Prox1. Our findings also indicate that HoxD8 plays crucial roles in the maturation and maintenance of lymphatic vessels, and suggest the possibility that HoxD8 can serve as a new therapeutic target in the treatment of inflammatory diseases, lymphedema, and lymphatic metastasis of tumors.

Materials and Methods

Cell culture and adenovirus infection

Maintenance, differentiation, culture and cell sorting of Tc-inducible MGZ5TcH2 ES cell lines were performed as described (Yamashita et al., 2000; Masui et al., 2005; Mishima et al., 2007). Briefly, VEGFR2-expressing endothelial progenitor cells derived from Tc-Empty or Tc-Prox1 ES cells were cultured in the absence or presence of Tc for 3 days. HUVECs and HDLECs were purchased from Sanko Junyaku and TaKaRa, and cultured in endothelial basal medium (EBM) containing 2% and 5% fetal bovine serum (FBS), respectively, supplemented with endothelial-cell growth supplement (TaKaRa). Recombinant adenoviruses encoding mouse Prox1 and HoxD8 were generated and used as described (Yamazaki et al., 2009). The *HoxD8* construct in the pSG5 vector was kindly provided by Vincenzo Zappavigna (University of Modena and Reggio Emilia, Italy). Purification of adenoviruses was performed using Virakit for adenovirus 5 (Virapur).

FACS analysis

We obtained LECs and BECs from mouse embryos as described previously (Hirashima et al., 2008). E14.5 mouse embryos, after removing their liver and spleen, were dissected and digested with 1.2 U/ml Dispase (Gibco), 50 μg/ml DNaseI (Roche) and 0.05% collagenase S-1 (Nitta Gelatin) to obtain single-cell suspension. After blocking Fc-receptors with an anti-mouse CD16/CD32 Fc receptor (FcR; PharMingen), all cells were stained with phycoerythrin (PE)-conjugated CD45 antibody (PharMingen) to sort CD45- non-hematopoietic cells using AutoMACS (Miltenyi Biotec). The cells were also stained with biotinylated anti-LYVE-1 antibody (ALY7; eBioscience) followed by allophycocyanin-conjugated streptoavidin (PharMingen) to visualize LYVE-1+ cells (LECs). The cells were also co-stained with a fluorescein isothiocyanate (FITC)-conjugated anti-PECAM-1/CD31 antibody (PharMingen) to visualize CD31+ cells (BECs). We sorted CD31+ LYVE-1- cells as BECs and CD31+ LYVE-1+ cells as LECs using FACS Vantage (Beckton Dickinson).

RNA isolation, and microarray and RT-PCR analyses

Total RNAs were extracted using the RNeasy Mini Kit (QIAGEN) to perform microarray and RT-PCR analyses. Oligonucleotide microarray analysis was performed using GeneChip Mouse Genome 430 2.0 Array (Affymetrix) according to the manufacturer's instructions. FileMaker Pro software (Filemaker) was used for statistical analysis. RNAs were reverse transcribed by random priming using Superscript III Reverse Transcriptase (Invitrogen). Expression of various Hox-family members was compared by RT-PCR analysis. PCR products were separated by electrophoresis in 1% agarose gel and visualized with ethidium bromide. Quantitative RT-PCR analysis was performed using the ABI PRISM 7500 Fast Real-Time PCR System (Applied Biosystems) and Power SYBR Green (Applied Biosystems). The primer sequences are shown in supplementary material Table S3.

RNA interference and oligonucleotides

siRNAs were introduced into cells using HiPerFect reagent (QIAGEN) according to the manufacturer's instructions. The target sequence for human *HoxD8* was 5′-UUUGUCUUCCUCUUCGUCUACCAGG-3′ (Stealth RNAi; Invitrogen), whereas that for human *Prox1* was 5′-CACCUUAUUCGGGAAGUGCAA-3′. Negative control was obtained from Invitrogen (Stealth RNAi Negative Control Med GC).

Immunohistochemistry, immunofluorescence microscopy and western blotting

Whole mounts of diaphragms were fixed with 10% neutral-buffered formalin for 1 hour at 4°C and washed overnight in phosphate-buffered saline (PBS) containing 10%, 15% and 20% sucrose at 4°C, followed by immunostaining. Immunostaining was carried out with anti-β-galactosidase (1:1000 dilution; Cappel) and anti-LYVE-1 (1:200 dilution; Abcam) antibodies. Stained specimens were examined using an LSM 510 META confocal microscope (Carl Zeiss). All images were imported into Adobe Photoshop as JPEGs or TIFFs for contrast manipulation and figure assembly. Antibodies to FLAG epitope and α-tubulin for western blot analysis were obtained from Sigma. Anti-Prox1 and -Ang-2 antibodies were from Chemicon and Abcam, respectively. Anti-human FoxC2 was described previously (Mani et al., 2007). Western blot analyses were performed as described (Watabe et al., 2003). The bound antibody was detected using a chemiluminescent substrate (ECL; Amersham) and a LAS-4000 Luminescent image analyzer (Fuji Photo Film).

Model of chronic aseptic peritonitis

BALB/c mice at 5 weeks of age, obtained from Charles River Laboratories, were used. The model of chronic aseptic peritonitis was described previously (Iwata et al., 2007). We intraperitoneally injected 2 ml of 3% thioglycollate medium (BBL thioglycollate medium, BD Biosciences) into BALB/c mice every 2 days for 2 weeks to induce peritonitis. Adenovirus encoding β-galactosidase or HoxD8 was also intraperitoneally injected twice per week during the same period. The mice were then

sacrificed, and their diaphragms excised and prepared for immunostaining as described above. Statistical analysis was performed using GraphPad Prism5 (GraphPad Software). Results were expressed as individual values and mean values ± s.e. Differences were evaluated by Mann-Whitney test and considered statistically significant at $P<0.05$. Plaques consisting of macrophages were obtained from the peritoneal surface of the diaphragm and treated with RNAlater (Ambion), followed by RNA isolation and quantitative RT-PCR analyses for VEGF-A, VEGF-C and VEGF-D.

Production of adenovirus

Recombinant adenoviruses encoding mouse Prox1 and HoxD8 were generated and used as described (Yamazaki et al., 2009). *Ang2* construct was kindly provided by Gou Young Koh (Korea Advanced Institute of Science and Technology, Republic of Korea).

Cell-proliferation assay

Cells were seeded at a density of 5×10^4 cells/well in 12-well plates and transfected with siRNAs using HiPerfect (QIAGEN). Cells were trypsinized and counted by a Coulter counter on day 2 after siRNA transfection. The experiments were performed in triplicate.

Chamber migration assay

Migration assay was performed as described previously (Mishima et al., 2007). As a chemoattractant, 100 ng/ml of recombinant VEGF-C (Calbiochem) were used.

We thank Vincenzo Zappavigna and Gou Young Koh for providing the *HoxD8* and *Ang2* plasmids, respectively, and all the members of the Department of Molecular Pathology of the University of Tokyo for discussion. This research was supported by KAKENHI (Grants-in-Aid for Scientific Research) from the Ministry of Education, Culture, Sports, Science and Technology of Japan.

References

Boudreau, N. J. and Varner, J. A. (2004). The homeobox transcription factor Hox D3 promotes integrin alpha 5 beta 1 expression and function during angiogenesis. *J. Biol. Chem.* **279**, 4862-4868.

Bruhl, T., Urbich, C., Aicher, D., Acker-Palmer, A., Zeiher, A. M. and Dimmeler, S. (2004). Homeobox A9 transcriptionally regulates the EphB4 receptor to modulate endothelial cell migration and tube formation. *Circ. Res.* **94**, 743-751.

Dellinger, M., Hunter, R., Bernas, M., Gale, N., Yancopoulos, G., Erickson, R. and Witte, M. (2008). Defective remodeling and maturation of the lymphatic vasculature in Angiopoietin-2 deficient mice. *Dev. Biol.* **319**, 309-320.

François, M., Caprini, A., Hosking, B., Orsenigo, F., Wilhelm, D., Browne, C., Paavonen, K., Karnezis, T., Shayan, R., Downes, M. et al. (2008). Sox18 induces development of the lymphatic vasculature in mice. *Nature* **456**, 643-647.

Gale, N. W., Thurston, G., Hackett, S. F., Renard, R., Wang, Q., McClain, J., Martin, C., Witte, C., Witte, M. H., Jackson, D. et al. (2002). Angiopoietin-2 is required for postnatal angiogenesis and lymphatic patterning, and only the latter role is rescued by Angiopoietin-1. *Dev. Cell* **3**, 411-423.

Hirashima, M., Sano, K., Morisada, T., Murakami, K., Rossant, J. and Suda, T. (2008). Lymphatic vessel assembly is impaired in Aspp1-deficient mouse embryos. *Dev. Biol.* **316**, 149-159.

Hong, Y. K., Harvey, N., Noh, Y. H., Schacht, V., Hirakawa, S., Detmar, M. and Oliver, G. (2002). Prox1 is a master control gene in the program specifying lymphatic endothelial cell fate. *Dev. Dyn.* **225**, 351-357.

Iwata, C., Kano, M. R., Komuro, A., Oka, M., Kiyono, K., Johansson, E., Morishita, Y., Yashiro, M., Hirakawa, K., Kaminishi, M. et al. (2007). Inhibition of cyclooxygenase-2 suppresses lymph node metastasis via reduction of lymphangiogenesis. *Cancer Res.* **67**, 10181-10189.

Izpisùa-Belmonte, J. C., Dollé, P., Renucci, A., Zappavigna, V., Falkenstein, H. and Duboule, D. (1990). Primary structure and embryonic expression pattern of the mouse Hox-4.3 homeobox gene. *Development* **110**, 733-745.

Johnson, N. C., Dillard, M. E., Baluk, P., McDonald, D. M., Harvey, N. L., Frase, S. L. and Oliver, G. (2008). Lymphatic endothelial cell identity is reversible and its maintenance requires Prox1 activity. *Genes. Dev.* **22**, 3282-3291.

Karpanen, T. and Alitalo, K. (2008). Molecular biology and pathology of lymphangiogenesis. *Annu. Rev. Pathol.* **3**, 367-397.

Mani, S. A., Yang, J., Brooks, M., Schwaninger, G., Zhou, A., Miura, N., Kutok, J. L., Hartwell, K., Richardson, A. L. and Weinberg, R. A. (2007). Mesenchyme Forkhead 1 (FOXC2) plays a key role in metastasis and is associated with aggressive basal-like breast cancers. *Proc. Natl. Acad. Sci. USA* **104**, 10069-10074.

Masui, S., Shimosato, D., Toyooka, Y., Yagi, R., Takahashi, K. and Niwa, H. (2005). An efficient system to establish multiple embryonic stem cell lines carrying an inducible expression unit. *Nucleic Acids Res.* **33**, e43.

Mishima, K., Watabe, T., Saito, A., Yoshimatsu, Y., Imaizumi, N., Masui, S., Hirashima, M., Morisada, T., Oike, Y., Araie, M. et al. (2007). Prox1 induces lymphatic endothelial differentiation via integrin α9 and other signaling cascades. *Mol. Biol. Cell* **18**, 1421-1429.

Oliver, G. (2004). Lymphatic vasculature development. *Nat. Rev. Immunol.* **4**, 35-45.

Pearson, J. C., Lemons, D. and McGinnis, W. (2005). Modulating Hox gene functions during animal body patterning. *Nat. Rev. Genet.* **6**, 893-904.

Petrova, T. V., Makinen, T., Makela, T. P., Saarela, J., Virtanen, I., Ferrell, R. E., Finegold, D. N., Kerjaschki, D., Yla-Herttuala, S. and Alitalo, K. (2002). Lymphatic endothelial reprogramming of vascular endothelial cells by the Prox-1 homeobox transcription factor. *EMBO J.* **21**, 4593-4599.

Petrova, T. V., Karpanen, T., Norrmén, C., Mellor, R., Tamakoshi, T., Finegold, D., Ferrell, R., Kerjaschki, D., Mortimer, P., Ylä-Herttuala, S. et al. (2004). Defective valves and abnormal mural cell recruitment underlie lymphatic vascular failure in lymphedema distichiasis. *Nature Med.* **10**, 974-981.

Shin, J. W., Min, M., Larrieu-Lahargue, F., Canron, X., Kunstfeld, R., Nguyen, L., Henderson, J. E., Bikfalvi, A., Detmar, M. and Hong, Y. K. (2006). Prox1 promotes lineage-specific expression of fibroblast growth factor (FGF) receptor-3 in lymphatic endothelium: a role for FGF signaling in lymphangiogenesis. *Mol. Biol. Cell* **17**, 576-584.

Srinivasan, R. S., Dillard, M. E., Lagutin, O. V., Lin, F. J., Tsai, S., Tsai, M. J., Samokhvalov, I. M. and Oliver, G. (2007). Lineage tracing demonstrates the venous origin of the mammalian lymphatic vasculature. *Genes Dev.* **21**, 2422-2432.

Tammela, T., Zarkada, G., Wallgard, E., Murtomäki, A., Suchting, S., Wirzenius, M., Waltari, M., Hellström, M., Schomber, T., Peltonen, R. et al. (2008). Blocking VEGFR-3 suppresses angiogenic sprouting and vascular network formation. *Nature* **454**, 656-660.

van den Akker, E., Fromental-Ramain, C., de Graaff, W., Le Mouellic, H., Brûlet, P., Chambon, P. and Deschamps, J. (2001). Axial skeletal patterning in mice lacking all paralogous group 8 Hox genes. *Development* **128**, 1911-1921.

Watabe, T., Nishihara, A., Mishima, K., Yamashita, J., Shimizu, K., Miyazawa, K., Nishikawa, S. and Miyazono, K. (2003). TGF-β receptor kinase inhibitor enhances growth and integrity of embryonic stem cell-derived endothelial cells. *J. Cell Biol.* **163**, 1303-1311.

Wigle, J. T. and Oliver, G. (1999). Prox1 function is required for the development of the murine lymphatic system. *Cell* **98**, 769-778.

Wigle, J. T., Harvey, N., Detmar, M., Lagutina, I., Grosveld, G., Gunn, M. D., Jackson, D. G. and Oliver, G. (2002). An essential role for Prox1 in the induction of the lymphatic endothelial cell phenotype. *EMBO J.* **21**, 1505-1513.

Xue, Y., Cao, R., Nilsson, D., Chen, S., Westergren, R., Hedlund, E. M., Martijn, C., Rondahl, L., Krauli, P., Walum, E. et al. (2008). FOXC2 controls Ang-2 expression and modulates angiogenesis, vascular patterning, remodeling, and functions in adipose tissue. *Proc. Natl. Acad. Sci. USA* **105**, 10167-10172.

Yamashita, J., Itoh, H., Hirashima, M., Ogawa, M., Nishikawa, S., Yurugi, T., Naito, M., Nakao, K. and Nishikawa, S. (2000). Flk1-positive cells derived from embryonic stem cells serve as vascular progenitors. *Nature* **408**, 92-96.

Yamazaki, T., Yoshimatsu, Y., Morishita, Y., Miyazono, K. and Watabe, T. (2009). COUP-TFII regulates the functions of Prox1 in lymphatic endothelial cells through direct interaction. *Genes Cells* **14**, 425-434.

Enhancement of vascular progenitor potential by protein kinase A through dual induction of Flk-1 and Neuropilin-1

Kohei Yamamizu,[1] Kyoko Kawasaki,[2] Shiori Katayama,[1] Tetsuro Watabe,[2] and Jun K. Yamashita[1,3]

[1]Laboratory of Stem Cell Differentiation, Stem Cell Research Center, Institute for Frontier Medical Sciences, Kyoto University, Kyoto; [2]Department of Molecular Pathology, Graduate School of Medicine, University of Tokyo, Tokyo; and [3]Center for iPS Cell Research and Application, Institute for Integrated Cell-Material Sciences, Kyoto University, Kyoto, Japan

Fine tuning of vascular endothelial growth factor (VEGF) signaling is critical in endothelial cell (EC) differentiation and vascular development. Nevertheless, the system for regulating the sensitivity of VEGF signaling has remained unclear. Previously, we established an embryonic stem cell culture reproducing early vascular development using Flk1 (VEGF receptor-2)$^+$ cells as common progenitors, and demonstrated that cyclic adenosine monophosphate (cAMP) enhanced VEGF-induced EC differentiation. Here we show that protein kinase A (PKA) regulates sensitivity of Flk1$^+$ vascular progenitors to VEGF signaling for efficient EC differentiation. Blockade of PKA perturbed EC differentiation and vascular formation in vitro and ex vivo. Overexpression of constitutive active form of PKA (CA-PKA) potently induced EC differentiation and vascular formation. Expression of Flk1 and Neuropilin-1 (NRP1), which form a selective and sensitive receptor for $VEGF_{165}$, was increased only in CA-PKA–expressing progenitors, enhancing the sensitivity of the progenitors to $VEGF_{165}$ by more than 10 times. PKA activation induced the formation of a $VEGF_{165}$, Flk1, and NRP1 protein complex in vascular progenitors. These data indicate that PKA regulates differentiation potential of vascular progenitors to be endothelial competent via the dual induction of Flk1 and NRP1. This new-mode mechanism regulating "progenitor sensitivity" would provide a novel understanding in vascular development and regeneration. (Blood. 2009;114:3707-3716)

Introduction

Vascular endothelial growth factor (VEGF) signaling is a key regulator of vascular development during embryogenesis as well as neovascularization in the adult.[1-3] Intensity of VEGF signaling is strictly controlled during vascular development through ligand-receptor interaction.[4,5] Flk1 (also designated as VEGF receptor-2) is tyrosine-phosphorylated much more efficiently than Flt1 (VEGF receptor-1) upon VEGF binding and is thought to be the major receptor in endothelial cells (ECs) for VEGF-induced responses.[6-8] Whereas Flk1-null mice die at embryonic day 8.5 (E8.5) to E9.5 with no organized blood vessels,[9] Flt1-null mice die at midgestation with vascular overgrowth and disorganization.[10,11] Flt1 tyrosine kinase–deficient homozygous mice, in which VEGF can bind to the cell-surface domain of Flt1 but cannot conduct kinase signaling, developed normal vessels and survived,[12] indicating that VEGF signal intensity on Flk1 is regulated by absorption of VEGF to the higher affinity receptor, Flt1. VEGF-A heterozygotes die early in gestation due to failure in vascular system formation.[13] On the other hand, 2- to 3-fold overexpression of VEGF-A from its endogenous locus results in aberrant heart development and lethality at E12.5 to E14,[14] indicating that strictly balanced VEGF function is important in normal embryogenesis.

Neuropilin-1 (NRP1) is a type 1 membrane protein, which is expressed in particular classes of developing neurons[15,16] and functions as a receptor for the class 3 semaphorins mediating semaphorin-elicited inhibitory axon guidance signals to neurons.[17,18] NRP1 is also expressed in ECs of blood vessels and endocardial cells of the heart.[15,16,19] NRP1, together with Flk1, forms a specific receptor for $VEGF_{165}$, an isoform of VEGF, and the Flk1-$VEGF_{165}$-NRP1 complex potently enhances Flk1 signaling.[20] Coexpression of NRP1 with Flk1 in cultured ECs enhanced $VEGF_{165}$ binding to Flk1 and VEGF-elicited mitogenic and chemotactic activities.[20] Overexpression of NRP1 in mouse embryos resulted in an excess production of blood vessels and malformed hearts.[15] NRP1-null mice die midway through gestation at E10.5 to E12.5 and exhibit defects in the heart, vasculature, and nervous system.[16] These findings indicate that NRP1 plays an important role in regulating vascular development, and Flk1/NRP1 system would be important for controlling VEGF signal intensity. However, the regulatory mechanisms of Flk1/NRP1 expression in vascular development are not fully elucidated.

In the early embryo and in differentiating embryonic stem (ES) cells, Flk1 expression marks a common progenitor for both blood and endothelium.[21-24] To elucidate the mechanisms underlying vascular development, we have developed a novel ES cell differentiation system that exhibits early vascular development using Flk1$^+$ cells as common progenitors for vascular cells.[25] ES cell–derived Flk1$^+$ cells can differentiate into both ECs and mural cells (MCs: vascular smooth muscle cells and pericytes) and form mature vascular-like structures in vitro. We recently reported that adrenomedullin/cyclic adenosine monophosphate (cAMP) pathway enhanced EC differentiation and induced arterial EC appearance from Flk1$^+$ progenitors.[26] In the present study, to further elucidate

Submitted December 19, 2008; accepted July 23, 2009. Prepublished online as *Blood* First Edition paper, August 25, 2009; DOI 10.1182/blood-2008-12-195750.

This article is a continuation of a previous report.[25,26]

The online version of the article contains a data supplement.

The publication costs of this article were defrayed in part by page charge payment. Therefore, and solely to indicate this fact, this article is hereby marked "advertisement" in accordance with 18 USC section 1734.

the mechanisms of EC differentiation from vascular progenitor cells, we examined roles of cAMP pathways in EC differentiation. Here we report that protein kinase A (PKA) activation remarkably enhanced EC differentiation and vascular formation from Flk1$^+$ vascular progenitors. PKA markedly increased the sensitivity of vascular progenitors to VEGF through dual up-regulation of Flk1 and NRP1 and played a pivotal role in EC differentiation. This new-mode molecular system regulating "progenitor sensitivity" would offer novel insights for vascular development as well as molecular targets for vascular regeneration strategies.

Methods

Generation of ES cells carrying an inducible expression unit in ROSA locus

Murine ES cell line (EStTA5-4), expressing tetracycline-transactivator protein and containing the puromycin resistance gene,[27] was a kind gift from Dr T. Era (Kumamoto University, Kumamoto, Japan). We generated an ES cell line (EStTA-ROSA) by inserting a knockin vector carrying loxP and mutant loxP, loxP511, recombination sites flanking neomycin-resistant and herpes simplex virus thymidine kinase (HSV-TK) genes (a kind gift from Dr K. Tanimoto [University of Tsukuba, Tsukuba, Japan] and Dr P. Soriano [Mt Sinai School of Medicine, New York, NY]) into ROSA locus[28] of EStTA5-4 (supplemental Figure 1A, available on the *Blood* website; see the Supplemental Materials link at the top of the online article). Neomycin (200 μg/mL)–resistant colonies were selected and homogenous insertion of the loxP sites into ROSA locus was confirmed by Southern blotting using DIG High Prime DNA Labeling and Detection Starter Kit II (Roche Diagnostics; supplemental Figure 1B-C). The probes were generated by polymerase chain reaction (PCR) amplification using the primer pair, 5′ probe: 5′-TTCAACAGGGATATCGCAAGG and 5′-AGCCTGGTAG-CAGGAAGATC, and Neo probe: 5′-CTCGACGTTGTCACTGAA and 5′-AAGAACTCGTCAAGAAGGCG.

Generation of ES cells for CA-PKA expression

cDNA for constitutive active form (CA)–PKA (a kind gift from Dr G. S. McKnight, University of Washington, Seattle, WA)[29] was introduced into the downstream region of tetracycline responsive element–regulatable cytomegalovirus promoter of Exchange vector (supplemental Figure 1A).

Stable ES cells that express the CA-PKA under the control of the tetracycline responsive element–regulatable cytomegalovirus promoter were generated by introduction of Exchange vectors and pBS185 (Cre expression vector) to EStTA-ROSA cells using mouse ES cells Nucleofector Kit (Amaxa Biosystems). Cells were then plated on 10-cm dishes containing 1 μg/mL doxycycline (Dox$^-$). After 1 day, the medium was changed to Dox$^-$ medium with 200 μg/mL hygromycin. After 10 days, the medium was changed to Dox$^+$ medium with 200 μg/mL hygromycin and 1 μg/mL ganciclovir. Total hygromycin- and ganciclovir-resistant colonies were collected and subjected to further studies.

Antibodies

Monoclonal antibodies for murine Flk1 (AVAS12) and murine vascular endothelial (VE)–cadherin (VECD1, for fluorescence-activated cell sorting [FACS]) were described previously.[24] Monoclonal antibodies for murine CD31 (1:500), VE-cadherin (for immunostaining, 1:200), and endothelial nitric oxide synthase (eNOS; 1:200) were purchased from BD Pharmingen. Monoclonal antibodies for murine α-smooth muscle actin (SMA; 1:1000) were from Sigma-Aldrich. Antibodies for SM22α (1:400) and calponin (1:500) were from Abcam. Polyclonal antibodies for murine Claudin-5 (1:100) were from Invitrogen. Polyclonal antibodies for murine VEGF and rat Neuropilin1 were from R&D Systems.

Cell culture

ES cell lines, D3, EStTA-ROSA, and CA-PKA–introduced EStTA-ROSA were maintained as described.[26] Induction of differentiation of these ES cell lines was performed using differentiation medium (DM; alpha minimal essential medium [MEM; Gibco] supplemented with 10% fetal calf serum [Japan Bioserum Co Ltd] and 5×10^{-5} M 2-mercaptoethanol [Gibco]) as previously described.[25,26] In brief, undifferentiated ES cells were cultured in the absence of leukemia inhibitory factor on collagen type IV–coated dishes (Becton Dickinson) at cell density 0.75 to 1×10^3 cells/cm^2 for 96 to 108 hours. Cultured cells were harvested and subjected to magnetic cell sorting (MACS) purification. Purified Flk1$^+$ cells were then plated onto type IV–coated dishes at cell density 0.75 to 1×10^4 cells/cm^2 in DM. After 3 days of Flk1$^+$ cell differentiation (Flk-d3), induced ECs were then examined by immunohistochemistry and flow cytometric analysis. Various reagents, human $VEGF_{165}$, $VEGF_{121}$ (R&D Systems), 8-bromoadenosine-3′:5′-cyclic monophosphate sodium salt (8bromo-cAMP; Nacalai Tesque), γ-secretase inhibitor, DAPT, PI3K inhibitor, LY294002, GSK3β inhibitor, Bio, Akt inhibitor, TAT-Akt-in, PKA inhibitor, PKI, H89, p38 inhibitor, SB202190, MEK inhibitor, PD98059, PKCαβ inhibitor, PKCη inhibitor, PKCζ inhibitor, H-Ras inhibitor, FTI-277 (Calbiochem), and phospholipase C (PLC) inhibitor, U73122 (Tocris Cookson Inc) were occasionally added to the Flk1$^+$ cell culture. (DAPT, LY294002, Bio, TAT-Akt-in, SB202190, PD98059, PKCαβ inhibitor, PKCη inhibitor, and PKCζ inhibitor did not inhibit cAMP effect.) Human $VEGF_{165}$ was used as the representative of VEGF isoforms unless stated otherwise. In serum-free culture, a defined medium, SFO3 (Sanko Junyaku; including insulin, transferrin, sodium selenite, and ethanolamine), was used instead of DM.[25]

Three-dimensional culture

Three-dimensional culture was performed as described previously.[25] Briefly, Flk1$^+$ cells (4×10^5 cells/mL) were incubated in DM with VEGF on uncoated Petri dishes for 16 hours to induce aggregation. Aggregates were resuspended in 2 × DM and mixed with an isovolume of collagen I-A gel (3 mg/mL; Nitta Gelatin). We plated 250 to 300 μL of this mixture onto a lucent insert disk, Cell disk (Sumitomo Bakelite), in 24-well dishes. After 30 minutes at 37°C to allow polymerization, we added 500 μL DM. To monitor vascular formation, collagen-embedded Flk1$^+$ cell aggregates were cultured in a temperature- and gas-controlled chamber (37°C, 5% CO_2), and phase-contrast images were acquired every 10 minutes with Metamorph software (Molecular Devices) for up to 5 days.

Cell sorting and flow cytometric analysis

After induction of Flk1$^+$ cells, cultured cells were harvested and stained with allophycocyanin (APC)–conjugated anti-Flk1 antibody (AVAS12).[24] Flk1$^+$ cells were sorted by auto MACS (Miltenyi Biotec) using anti-APC MicroBeads (Miltenyi Biotec). At Flk-d3, cultured cells were harvested and stained with monoclonal antibodies for phycoerythrin-conjugated CD31 (Mec13.3; BD Pharmingen) together with APC-conjugated VECD1 or biotin-conjugated CXCR4 (BD Pharmingen) followed by streptavidin-conjugated APC (BD Pharmingen) or AVAS12, then subjected to analysis by FACSVantage or FACSAria (Becton Dickinson).

Immunocytochemistry

Immunostaining for cultured cells was carried out as described.[25,26] Briefly, 4% paraformaldehyde-fixed cells were blocked by 1% skim milk (BD Biosciences) and incubated overnight with primary antibodies at 4°C. For immunohistochemistry, anti–rat immunoglobulin G (IgG) conjugated with alkaline phosphatase and anti–mouse IgG horseradish peroxidase (Invitrogen) were used as secondary antibodies. For immunofluorescent staining, anti–mouse, –rat, –rabbit, or –goat IgG antibodies conjugated with Alexa488 or Alexa546 (Invitrogen) were used for secondary antibodies. Nuclei were visualized with DAPI (4,6 diamidino-2-phenylindole; Invitrogen). Double staining for NRP1 and CD31 was performed using anti-NRP1 antibody (1:100; R&D Systems) as first antibody, followed by secondary antibody, Alexa Fluor 488–conjugated donkey anti–goat IgG (1:500; Molecular Probes). CD31$^+$ cells were visualized using phycoerythrin-

conjugated anti-CD31 antibody (1:300; BD Pharmingen). Stained cells were photographed with inverted fluorescent microscopy, Eclipse TE2000-U (Nikon) and digital camera system AxioCam HRc with the use of AxioVision Software (Carl Zeiss), or confocal fluorescent microscopy (TCS SP2; Leica).

Immunostaining for three-dimensional culture

Immunostaining for vascular structures in type I collagen gel was performed after the whole-mount immunostaining procedure as described.[25] In brief, gels were fixed with 4% paraformaldehyde and blocked by 1% skim milk/0.1% Triton X/phosphate-buffered saline solution and incubated with anti-CD31 (BD Pharmingen) and anti–α smooth muscle actin (αSMA; Sigma-Aldrich), or anti-NRP1 (R&D Systems) and anti-Flk1 antibodies (1:200). Alexa Fluor 488–conjugated anti–mouse or anti–goat IgG and Alexa Fluor 567–conjugated anti–rat IgG (1:500; Zymed) were used as secondary antibodies. Alternatively, anti–rat IgG conjugated with alkaline phosphatase and anti–mouse IgG conjugated with horseradish peroxidase (Zymed) were used as secondary antibodies for enzymatic color development.

Cross-section of three-dimensional culture and immunostaining

Gel clots including vascular structure were fixed in 3.7% formaldehyde for 24 hours. Paraffin-embedded gel clots were sectioned at 3-μm thickness. The sections were mounted on glass slides coated with 2% 3-aminopropyl triethoxy silane (Tokyo Kasei). After deparaffinization and washing in distilled water, hematoxylin-eosin or immunohistochemical staining was performed.[30] For double immunostaining for CD31 and SMA, CD31 was first stained with whole-mount in-gel staining using anti-CD31 antibody and anti–rat IgG antibody conjugated with horseradish peroxidase. Subsequently, gel clots were subjected to paraffin embedding. Anti-SMA antibody (1:100; DAKO) was applied to sectioned slides overnight at 4°C. They were incubated with biotinylated horse anti–mouse serum diluted to 1:300 followed by streptavidin-alkaline phosphatase.

RNA isolation, RT-PCR, and quantitative RT-PCR

Total RNA was isolated from cells in Dox treatment or Dox-free condition at Flk-d3 using RNeasy (QIAGEN), according to the manufacturer's instructions. Reverse-transcription was performed with the SuperScript III first-strand synthesis system (Invitrogen). Reverse-transcription (RT)–PCR was carried out as described[26] using indicated primers (supplemental Table 1). Quantitative RT-PCR was performed using Power SYBR Green PCR Master Mix (Applied Biosystems) and StepOnePlus system (Applied Biosystems). The amount of target RNA was determined from the appropriate standard curve and normalized relative to the amount of *Gapdh* mRNA. Primer sequences are shown in supplemental Table 2.

Immunoprecipitation and immunoblotting

Immunoprecipitation and immunoblotting were performed according to the report by Pan et al.[31] In brief, Flk1$^+$ cells were incubated with vehicle, anti-VEGF (5 μg/mL), or anti-NRP1 antibodies (5 μg/mL; R&D Systems) in serum-free medium, SFO3 (Sanko Junyaku),[25] for 30 minutes at 37°C. Cells were then cooled on ice for 15 minutes, and VEGF isoforms were added, followed by 30-minute incubation at 4°C. Cells were stimulated for 7 minutes at 37°C and then washed with ice-cold phosphate-buffered saline and lysed in lysis buffer. Cell lysates were subjected to immunoprecipitation using Protein G HP SpinTrap (GE Healthcare) and anti-Flk1 antibody, and immunoblotted with antibodies specific for NRP1 (R&D Systems). Samples were run on sodium dodecyl sulfate/polyacrylamide gel electrophoresis using gradient gel (Atto Co) followed by electrophoretic transfer onto nitrocellulose membranes. After the blots were incubated for 1 hour in blocking agents Blocking One (Nacalai Tesque), they were incubated overnight with the respective NRP1 antibodies (0.5 μg/mL; R&D Systems). Horseradish peroxidase–conjugated anti–goat antibody (Zymed Laboratories) was used as secondary antibody (1:1000). Can Get Signal Immunoreaction Enhancer solution kit (Toyobo) was used for signal enhancement. Immunoreactivity was detected with the enhanced chemiluminescence kit Chemi-Lumi One (Nacalai Tesque).

Ex vivo whole-embryo culture

Embryos were dissected out of the deciduum and placed in 500 μL dimethyl ether containing 50% rat IC serum (Charles River Laboratories), 5 mM nonessential amino acids, 50 mM sodium pyruvate, and 27.5 mM 2-mercaptoethanol, pre-equilibrated at 37°C with 5% CO_2. Embryos were cultured at 37°C with 5% CO_2 and analyzed. H89 (dissolved in dimethyl sulfoxide) was used at 30 μM. The concentration of dimethyl sulfoxide was set at 0.3% in all cultures.[32] Whole-mount staining of embryos and yolk sacs was performed as described previously,[33] and microscopy was performed using a microscope (MZ6; Leica) with 5× objectives (Leica 10411589). Images were imported using Adobe Photoshop software, and quantification of whole yolk sacs and CD31-stained areas was performed using ImageJ software (National Institutes of Health). Results of quantification were expressed as ratio of CD31$^+$/whole yolk sac area, which provides an estimate of the proportion of the yolk sacs that were occupied by CD31-stained vascular structures. Animal experiments were done under the approval of the Animal Research Committee of Kyoto University in accordance with the guidelines for animal experiments in the Guide for the Care and Use of Laboratory Animals in Japan.

Statistical analysis

At least 3 independent experiments were performed. Statistical analysis of the data was performed with the Student *t* test or analysis of variance. *P* values less than .05 was considered significant. Values are reported as means plus or minus SD.

Results

cAMP/PKA pathway plays a critical role in vascular development

In our ES cell differentiation system, first we induced Flk1$^+$ progenitor cells from undifferentiated ES cells. Flk1$^+$ cells that appeared after 96 to 108 hours of differentiation of undifferentiated ES cells were negative for EC markers, such as CD31 and VE-cadherin.[24-26] Then, purified Flk1$^+$ progenitor cells were cultured for further differentiation to vascular cells. As previously reported, whereas no CD31$^+$ ECs appeared when Flk1$^+$ cells were cultured for 3 days with DM ("Methods") alone, addition of VEGF to the Flk1$^+$ cell culture induced selective appearance of CD31$^+$ ECs and SMA$^+$ MCs (Figure 1A).[25,26] Almost all of CD31$^+$ cells were also positive for other EC markers, VE-cadherin, claudin-5, and eNOS (Figure 1A-B).[25,26] SMA$^+$ MCs, which were reciprocally negative for EC markers (Figure 1B), expressed other smooth muscle cell markers, SM22α and calponin (Figure 1A). In this culture condition, only these 2 cell types (ie, ECs and MCs), and no blood cells such as CD45$^+$ cells, were specifically induced from Flk1$^+$ cells (Figure 1C).[26]

Stimulation of cAMP signaling by addition of 8bromo-cAMP, an analog of cAMP, together with VEGF substantially enhanced CD31$^+$ EC induction from Flk1$^+$ cells (Figure 2A-B). Similar to ECs induced by VEGF alone (Figure 1), CD31$^+$ ECs that appeared by treatment of 8bromo-cAMP and VEGF were also positive for other EC markers, VE-cadherin, eNOS, and claudin5, but not CD45 (supplemental Figure 2). Compared with VEGF alone, VEGF with 8bromo-cAMP induced approximately 2-fold increase in EC population (CD31$^+$ cells: 26.5% ± 2.3% in VEGF alone vs 52.3% ± 2.7% in VEGF with 8bromo-cAMP, n = 16; $P < .001$; Figure 2C). Total EC numbers induced from the same number of Flk1$^+$ cells were similarly increased approximately 2.3 times by 8bromo-cAMP treatment (CD31$^+$ cells: 9.4 ± 0.8 [× 10^4] cells in VEGF alone vs 21.8 ± 0.9 [× 10^4] cells in VEGF with 8bromo-cAMP; n = 4; $P < .001$; Figure 2D). PKA inhibitors, PKI and

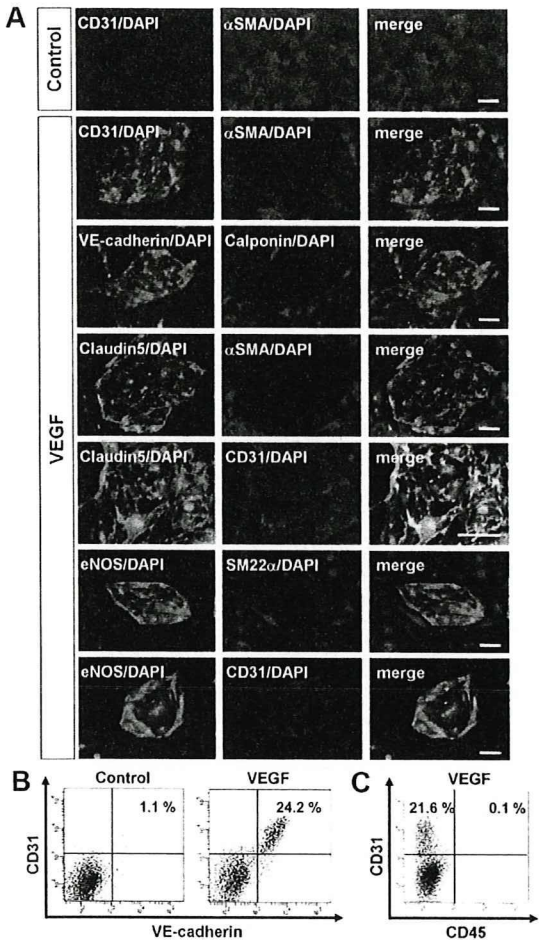

Figure 1. Vascular endothelial growth factor induces endothelial cells from vascular progenitors. (A-C) Cells after three-dimensional culture of Flk1$^-$ cells (Flk-d3). (A-B) Exclusive induction of endothelial cells (ECs) and mural cells (MCs) from Flk1$^-$ cells. (A) Expression of EC and MC markers. (Top panels) Double immunostaining of CD31 (green) and αSMA (red) cultured with differentiation medium (DM) alone (control). Note that no CD31$^+$ cells appeared. (Other panels) Vascular endothelial growth factor (VEGF) treatment (50 ng/mL). EC sheets appeared. Double staining with pan-EC markers (CD31, VE-cadherin, Claudin5, or eNOS; green) and MC markers (αSMA, SM22α, or Calponin; red). (Bottom panels) Double staining with eNOS (green) and CD31 (red). ECs and MCs were exclusively induced. Nuclei are stained with DAPI (blue). Scale bar represents 50 μm. (B) Flow cytometry. x-axis: VE-cadherin; y-axis: CD31. Percentages of CD31$^+$/VE-cadherin$^+$ ECs in total Flk1$^+$ cell–derived cells are indicated. (C) Flow cytometry. x-axis: CD45; y-axis: CD31. Percentages of CD31$^+$/CD45$^-$ ECs and CD31$^+$/CD45$^+$ blood cells in total Flk1$^+$ cell–derived cells are indicated. Note that almost no CD45$^+$ cells were induced in this culture.

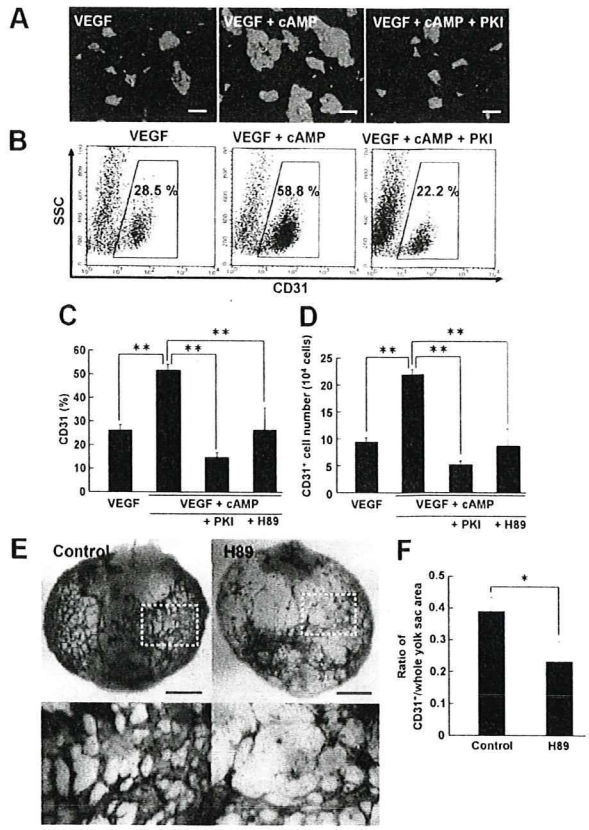

Figure 2. Cyclic adenosine monophosphate/protein kinase A pathway plays a critical role in vascular development. (A-D) Enhancement of EC induction by cyclic adenosine monophosphate (cAMP) through protein kinase A (PKA) at Flk-d3. (A) Fluorescent staining for CD31 (green). (Left panel) VEGF treatment alone (50 ng/mL). (Middle panel) VEGF with 8bromo-cAMP (0.5 mM). (Right panel) VEGF with 8bromo-cAMP and PKA inhibitor, PKI (10 μM). Nuclei are stained with DAPI (blue). Scale bars represent 250 μm. (B) Flow cytometry. x-axis: CD31; y-axis: side scatter (SSC). Percentages of CD31$^+$ ECs in total Flk1$^+$ cell–derived cells are indicated. (C-D) Quantitative evaluation of the effect of PKA inhibitors on CD31$^+$ EC induction from Flk1$^+$ cells by FACS. (C) Percentages of CD31$^+$ cell population in total Flk1$^+$ cell–derived cells. VEGF (50 ng/mL; n = 16); VEGF and 8bromo-cAMP (0.5 mM; n = 16); VEGF, cAMP, and PKI (10 μM; n = 7); and VEGF, cAMP, and H89 (10 μM; n = 6) treatment are shown (**$P < .01$ vs VEGF and 8bromo-cAMP). (D) CD31$^+$ cell number that appeared from 1.5×10^5 Flk1$^+$ cells. VEGF (50 ng/mL; n = 4); VEGF and 8bromo-cAMP (0.5 mM; n = 4); VEGF, cAMP, and PKI (10 μM; n = 4); and VEGF, cAMP, and H89 (10 μM; n = 4) treatment are shown (**$P < .01$ vs VEGF and 8bromo-cAMP). (E-F) Role of PKA in vascular formation in the embryo. (E) Representative results of ex vivo culture of mouse embryo. Isolated E6.75 concepti were cultured in the absence (control, left panels) or presence (right panels) of H89 (30 μM) for 3 days. Vasculature in yolk sacs of concepti was immunostained for CD31 (purple). Bottom panels correspond to boxed regions in control and H89, respectively. Apparent reduction of CD31$^+$ vascular formation was induced by H89 treatment. Scale bar represents 1 mm. (F) Quantitative evaluation of CD31$^+$ vasculature formation in yolk sacs of concepti. The ratio of CD31$^+$/whole yolk sac area was evaluated (n = 3; *$P < .05$ vs control).

H89, but not many other kinase inhibitors ("Methods"), specifically inhibited the cAMP effects on EC induction (Figure 2A-D). These results indicated that the cAMP/PKA pathway specifically enhances the effect of VEGF on EC differentiation from Flk1$^+$ progenitor cells.

We further examined the role of PKA in vascular development with ex vivo whole-embryo culture assay. Embryonic day 6.75 concepti were picked out from the uteri of pregnant mice and cultured for 3 days, during which CD31$^+$ blood vessels were formed in the yolk sac. Using this system, we could examine early phase of EC differentiation ex vivo. In the presence of H89 during ex vivo culture, formation of blood vessels, which were evaluated by CD31 staining, in yolk sac was markedly disturbed, showing malformation of vascular networks with decrease in the caliber size and CD31$^+$ areas (Figure 2E). Indeed, CD31$^+$ area within whole yolk sac area was significantly decreased in H89-treated embryo to approximately 59% of that in control (n = 3; $P = .025$; Figure 2F). These results indicate that PKA also plays an important role in early vascular development in vivo.

CA-PKA enhanced EC differentiation and vascular formation from Flk1$^+$ vascular progenitors

To dissect PKA function in EC differentiation, we generated ES cells expressing CA-PKA by tetracycline-regulatable system (Tet-Off; supplemental Figure 1). Although negative effects of high-dose Dox (~ 25 μg/mL) on EC differentiation, proliferation, and survival were

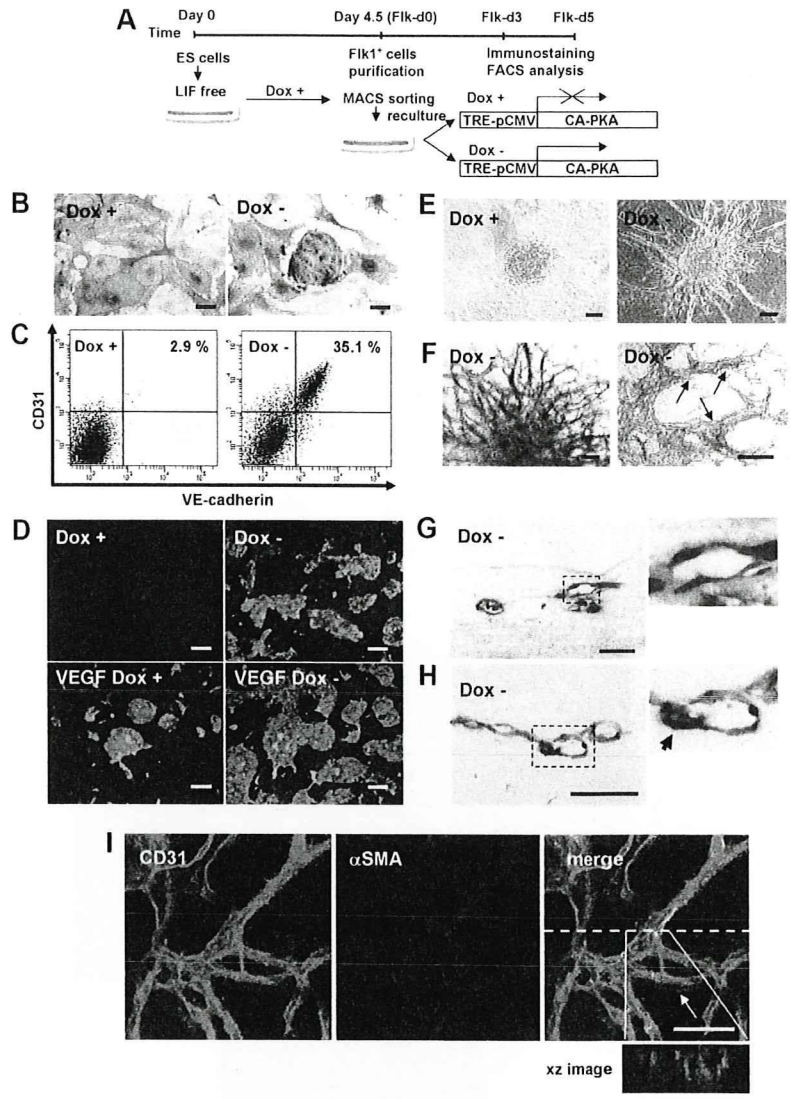

Figure 3. CA-PKA enhances EC differentiation from Flk1$^+$ vascular progenitors. (A) Experimental system for PKA activation. An embryonic stem (ES) cell line expressing constitutive active (CA) form of PKA by tetracycline-inducible expression system (Tet-Off) was established. Doxycycline (Dox) was added during the first 4.5-day culture of ES cell differentiation to Flk1$^+$ cells. Flk1$^+$ cells were sorted by magnetic cell sorting (MACS) and subjected to two-dimensional culture on collagen-coated dishes or three-dimensional culture in collagen gel, and were cultured in the presence or absence of Dox (1 μg/mL). (B-D) Two-dimensional culture with DM, at Flk-d3. (B) Double immunostaining for CD31 (purple) and αSMA (brown). (Left panel) Dox (1 μg/mL) treatment. (Right panel) Dox-free. Culture with DM alone. Scale bar represents 100 μm. (C) Flow cytometry for EC markers, CD31 and VE-cadherin. Percentages of CD31$^+$/VE-cadherin$^+$ ECs in total Flk1$^-$ cell–derived cells are indicated. (D) Fluorescent staining for CD31 (green) and DAPI (blue). (Left panels) Dox (1 μg/mL) treatment. (Right panels) Dox-free. Flk1$^-$ cells stimulated with vehicle (top panels) or VEGF (50 ng/mL; bottom panels). Scale bars represent 250 μm. (E-I) Three-dimensional culture of Flk1$^+$ cell aggregates in type I collagen gel with DM alone. (E) Phase-contrast images after 5-day culture. (Left panel) Dox (1 μg/mL) treatment. (Right panel) Dox-free. Scale bars represent 100 μm. (F) In-gel double immunostaining for CD31 (purple) and αSMA (brown) in Dox-free condition. (Left panel) Gross appearance of vascular structure. (Right panel) Higher magnification view. αSMA$^+$ cells attached to CD31$^+$ EC tube structure are observed (arrows). Scale bars represent 100 μm. (G-H) Cross-section of three-dimensional culture in Dox-free condition. (G) Hematoxylin-eosin staining. (H) Double immunostaining for CD31 (brown) and αSMA (red). Right panels correspond to boxed regions. Scale bars represent 250 μm. αSMA$^+$ cell attached to CD31$^+$ EC tube structure is observed (arrow). (I) Confocal microscopic analysis of vascular structure. Double fluorescent staining for CD31 and αSMA in Dox-free condition. (Left panel) CD31 (green). (Middle panel) αSMA (red). (Right panel) Merged image. αSMA$^-$ cell attached to CD31$^-$ EC tube structure is observed (arrow). CD31$^+$ cells formed true lumen (green) with attached mural cells (red) shown in xz image. Dashed line indicates sliced position. Scale bars represent 100 μm.

reported,[34] lower concentration of Dox (1 μg/mL) did not affect EC appearance in control ES cells (EStTA-ROSA; supplemental Figure 3). We induced differentiation of ES cells in the presence of Dox for 4.5 days, and purified Flk1$^+$ cells were recultured on type IV collagen–coated dishes with DM alone in the presence or absence of Dox (Figure 3A). In the presence of Dox (Dox$^+$), only SMA$^+$ mural cells, but not ECs were induced (Figure 3B-C), compatible with our previous results[25] (Figure 1A-B). Surprisingly, considerable amounts of CD31$^+$ ECs were generated even in the absence of VEGF when CA-PKA expression was induced by the depletion of Dox (Dox$^-$; Figure 3B; supplemental Videos 1-2). Almost all of CA-PKA–induced CD31$^+$ cells on 2-dimensional culture condition were also positive for VE-cadherin, eNOS, and claudin5 (Figure 2C, supplemental Figure 4). CD31$^+$/VE-cadherin$^+$ cells observed in CA-PKA–activated condition were positive for SMA, SM22α, and calponin (supplemental Figure 4). When we tested the effects of CA-PKA with VEGF, EC appearance with VEGF in Dox$^+$ condition was further enhanced by expression of CA-PKA (Figure 3D). These results indicate that PKA should enhance EC differentiation from vascular progenitors.

We further examined vascular formation from Flk1$^+$ cells in three-dimensional culture[25] to investigate PKA function in vascular development. When aggregates of Flk1$^+$ cells were cultured in type I collagen gel with DM alone, no sprouting of vessels was observed in Dox$^+$ condition. In contrast, CA-PKA expression (Dox$^-$) induced vascular-like structure formation even in the absence of VEGF (Figure 3E; supplemental Video 3). In-gel immunostaining showed the vascular-like structure consisted of CD31$^+$ ECs with surrounding SMA$^+$ mural cells (Figure 3F). Cross-sections revealed true lumens with CD31$^+$ ECs and attached SMA$^+$ MCs (Figure 3G-H). Confocal microscopic study further showed vascular-like structure formation with EC tube and mural cell attachment (Figure 3I). In addition, PKA activation induced CD45$^+$ blood cells within the vascular lumen (supplemental Figure 5A). Occasionally, beating cardiomyocytes, which were positive for cardiac troponin T, were observed along with vascular structures (supplemental Figure 5B; supplemental Video 4). PKA, thus, should play an important role in vascular development through enhancement of EC differentiation.

Dual up-regulation of Flk1 and NRP1 was induced by PKA

Next, we investigated the molecular mechanism of the PKA effects in EC differentiation and vascular development. First we examined PKA activity in vascular progenitor cells. Whereas PKA activity was significantly increased by addition of 8bromo-cAMP, VEGF treatment did not induce PKA activation (supplemental Figure 6),

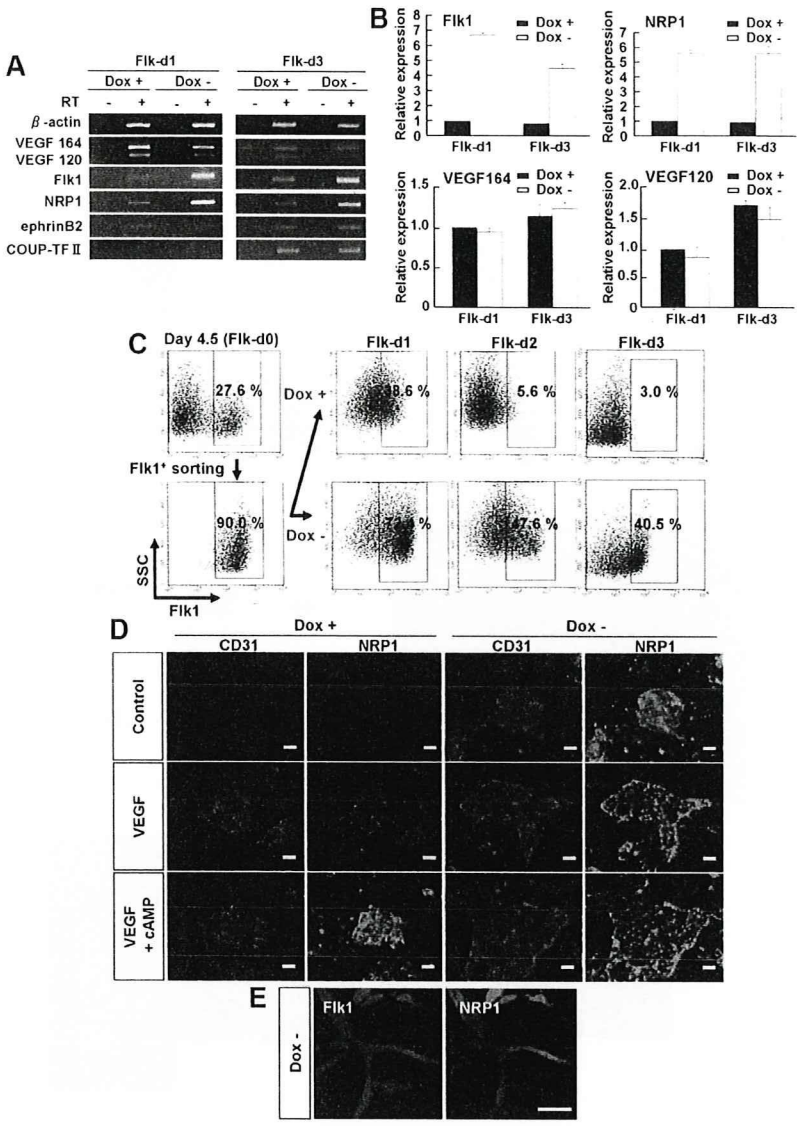

Figure 4. Dual up-regulation of Flk1 and NRP1 by PKA activation. (A-D) Two-dimensional culture of Flk1$^-$ cells. (A) RT-PCR showing mRNA expression of $VEGF_{164}$, $VEGF_{120}$, Flk1, NRP1, ephrinB2 (arterial marker), and COUP-TF II (venous marker) after 1 (Flk-d1) and 3 (Flk-d3) days of culture of Flk1$^-$ cells with DM alone in the presence or absence of Dox (1 μg/mL). (B) Quantitative RT-PCR showing mRNA expression of Flk1, NRP1, $VEGF_{164}$, and $VEGF_{120}$ at Flk-d1 and Flk-d3 in the presence or absence of Dox. mRNA expression at Flk-d1 with Dox was set as 1.0. (C) Time course of Flk1$^+$ cell appearance evaluated by FACS. Flk1$^+$ cell appearance was examined on differentiation day 4.5 before and after sorting, and at Flk-d1, Flk-d2, and Flk-d3 cultured with DM alone in the presence or absence of Dox (1 μg/mL). (Top panels) Dox treatment. (Bottom panels) Dox-free. Percentages of Flk1$^+$ cells are indicated. (D) Double fluorescent staining for CD31 and NRP1 at Flk-d3. (Left 6 panels) Dox treatment. (Right 6 panels) Dox-free. Flk1$^+$ cells stimulated with vehicle (top panels), VEGF (50 ng/mL; middle panels), or VEGF and 8bromo-cAMP (0.5 mM; bottom panels). Scale bars represent 100 μm. (E) Vascular formation from Flk1$^+$ cell aggregates in three-dimensional culture in Dox-free condition at Flk-d5. In-gel double fluorescent staining for Flk1 and NRP1. (Left panel) Flk1 (red). (Right panel) NRP1 (green). Scale bars represent 100 μm.

indicating that PKA pathway did not work downstream of VEGF signaling in vascular progenitor cells. In addition, activation of PKA by induction of CA-PKA in Flk1$^+$ cells did not increase VEGF mRNA expression (Figure 4A-B). These results indicate that PKA signaling did not enhance VEGF signaling through the formation of a positive feedback loop between VEGF and PKA. In contrast, overexpression of CA-PKA up-regulated Flk1 and NRP1 mRNA expression from the early stage of Flk1$^+$ cell culture (ie, at days 1 and 3 after Flk1 sorting; Figure 4A). Arterial EC marker, ephrinB2,[35,36] and venous EC marker, COUP-TF II,[37] were not affected by CA-PKA expression (Figure 4A). Quantitative RT-PCR analysis revealed that PKA activation induced approximately 5- to 7-fold increase in Flk1 and NRP1 mRNA expression in total cells at Flk-d1 and Flk-d3 (Figure 4B). Similar significant up-regulation of Flk1 and NRP1 mRNA expression was observed in 8bromo-cAMP–treated Flk1$^+$ cells (supplemental Figure 7A). We further confirmed the time course of Flk1 protein expression in the early stage of Flk1$^+$ cell culture by FACS. When purified Flk1$^+$ progenitor cells were cultured in the absence of VEGF, Flk1 expression was rapidly decreased and lost within 3 days, compatible with our previous results[25] (Figure 4C top panels). On the other hand, when CA-PKA was induced in purified Flk1$^+$ cells, Flk1 expression was essentially maintained, even in the absence of VEGF. At Flk-d1, almost all Flk1$^+$ cells were still negative for EC markers, CD31 and VE-cadherin (supplemental Figure 8), indicating that PKA should work at the progenitor stage to enhance EC appearance from Flk1$^+$ progenitor cells. As for NRP1 protein expression, whereas clear up-regulation of NRP1 expression was observed only in VEGF with 8bromo-cAMP treatment in Dox$^-$ condition, CA-PKA activation (Dox$^-$) induced NRP1 expression even in the absence of VEGF at Flk-d3 (Figure 4D). Furthermore, Flk1 and NRP1 were also coexpressed in vascular structure in vitro induced with CA-PKA expression (Figure 4E). These results suggest that PKA pathway should enhance EC differentiation and vascular formation through dual induction of Flk1 and NRP1.

Sensitivity of VEGF signaling is markedly enhanced by PKA

To precisely define the biologic function of up-regulated Flk1 and NRP1 by PKA activation, we tested dose-response effects of